Technical report; TR 214

KNMI

The Implementation of two Mixed-Layer Schemes in the HOPE Ocean General Circulation Model

M. van Eijk

Koninklijk Nederlands Meteorologisch Instituut

december 1998

Technical report = Technisch rapport; TR 214

De Bilt, 1998

P.O. Box 201
3730 AE De Bilt
Wilhelminalaan 10
Telephone +31 30 220 69 11
Telefax +31 30 221 04 07

Contact person for this report: G. Burgers

UDC: 551.465.5
681.3.06
551.509.313

ISSN: 0169-1708

ISBN: 90-369-2152-X

Technical report; TR 214

The Implementation of two Mixed-Layer Schemes in the HOPE Ocean General Circulation Model

M. van Eijk

december 1998

Abstract

Two mixed-layer schemes are implemented in the HOPE Ocean General Circulation Model that is used at the European Centre for Medium-Range Weather Forecasts (ECMWF). They are a nonlocal diffusion (NLD) scheme based on the KPP model by Large et al. (1994), and a bulk mixed-layer (BML) scheme based on the model by Sterl and Kattenberg (1994), The aim of the implementation was to embed the mixed-layer schemes in the HOPE model with minor modifications to the original code. By setting a single switch one can choose one of the new mixed-layer schemes or the original HOPE mixing scheme.

Results with the mixed-layer schemes show improved global sea surface temperature fields in the case of the BML scheme and the formation of barrier layers in the case of the NLD model. Computational costs increase by an amount of 12% and 30% for the BML and the NLD scheme respectively.

Samenvatting

Twee menglaagmodellen zijn geïmplementeerd in het HOPE oceaanmodel dat op het Europese Centrum voor Weersverwachtingen op Middellange Termijn (ECMWF) gebruikt wordt: een niet-lokaal diffusiescheme (NLD) gebaseerd op het KPP-model van Large et al. (1994), en een bulk menglaagschema (BML) model gebaseerd op het model van Sterl en Kattenberg (1994). Het doel van de implementatie was om deze menglaagmodellen in het HOPE model op te nemen met zo min mogelijk veranderingen in de broncode. Met een enkele parameter kunnen deze nieuwe menglaagschema's of het oorspronkelijke HOPE mengschema gekozen worden.

Resultaten met de nieuwe menglaagschema's geven betere zeewateroppervlaktetemperaturen in het BML schema, en de formatie van 'barrier layers' in het NLD model. De rekenkosten nemen 12% en 30% toe voor het BML respectievelijk NLD schema.

Contents

1 Introduction *1*

2 Model physics *3*
2.1 The bulk mixed-layer scheme *3*
2.2 The nonlocal diffusion scheme *3*
2.3 The original HOPE scheme *4*

3 Numerical implementation *5*
3.1 Mixed-layer schemes in HOPE *5*
3.2 The nonlocal diffusion scheme *6*
3.2.1 Calling conventions 6
3.2.2 The first pass 6
3.2.3 The second pass 9
3.3 The bulk mixed-layer scheme *10*

4 Some results *13*
4.1 Model initialization and forcing *13*
4.2 Surface fields *13*
4.3 Thermocline structure *16*
4.4 The barrier layer *18*
4.5 Discussion *19*

Bibliography *21*

A List of variables *22*

B Modifications to HOPE routines *24*

1. Introduction

The interface of the ocean and atmosphere is formed by the two planetary boundary layers, which have complex interactions. In the modelling of the ocean-atmosphere system, the challenge for an ocean boundary-layer scheme is to give a true to nature representation of the upper-ocean structure. One of the key parameters in this context is the sea-surface temperature (SST). A major difficulty one encounters in implementing a boundary-layer scheme in an ocean general circulation model (OGCM) is the vast range of length and time scales of the system. For example, the vertical resolution of an OGCM is restricted to 5–20 m, which is far too low to represent the small scale turbulence processes in the oceanic boundary layer. Therefore a suitable subgrid scale parameterization is desirable, which on the one hand is simple enough to be used in simulations of large-scale ocean circulation and on the other hand is able to reproduce the main physical boundary-layer characteristics.

Several types of subgrid parameterizations have been developed. Higher-order closure models (Mellor and Yamada, 1982), nonlocal mixing models (Large et al., 1994) and bulk mixed-layer models (Niiler and Kraus, 1977) are examples of models with varying amounts of physics incorporated. Choosing between schemes of this kind is balancing between the more complete physics of the elaborate models and the low computational costs of the simple models. For some purposes, simple models are appropriate, whereas elaborate boundary models are too inefficient and complex.

This document describes the implementation of two mixed-layer schemes in the version of the HOPE model (Hamburg Ocean with Primitive Equation) currently running at the ECMWF. The schemes are a bulk mixed-layer scheme as described by Sterl and Kattenberg (1994) and a nonlocal diffusion scheme as described by Large et al. (1994). The manual starts with a short description of the physics of the mixed-layer schemes. For an elaborate description of the HOPE model we refer to the HOPE manual, Wolff et al. (1997). In section 3 the technical details of the implementation in the HOPE model are discussed, together with a comprehensive description of the various subroutines that make up the two mixed-layer schemes. Finally, section 4 gives an overview of some results of experiments with the HOPE model with the mixed-layer schemes implemented. Appendix A gives a list of all new model variables and parameters used in the mixed-layer schemes. Again, for a complete list of HOPE variables and parameters we refer to the HOPE manual, Wolff et al. (1997). Appendix B lists the modified subroutines for the computation of the surface fluxes and ocean forcing.

2. Model physics

In this section the two new ocean mixed-layer schemes are described: the nonlocal diffusion parameterization scheme for the oceanic boundary layer of Large et al. (1994), and the bulk mixed-layer scheme of Sterl and Kattenberg (1994). Also the original mixed-layer scheme in the HOPE model is described briefly. An important parameter determined by the schemes is the depth of the layer in which the effects of mixing by turbulence are relevant. The two schemes utilize different concepts for this layer, respectively the boundary layer and the mixed layer. The boundary-layer depth is defined as the depth to which eddies are able to penetrate the stratified fluid, whereas the mixed-layer depth is the depth at which properties diverge from uniformity. The actual depth of the layers are found to be rather similar in most situations and is termed mixed-layer depth throughout this document. For a more comprehensive discussion of the mixed-layer schemes for a one dimensional case we refer to van Eijk et al. (1997).

2.1 The bulk mixed-layer scheme

The bulk mixed-layer scheme, based on a Niiler and Kraus (1977) type scheme, assumes uniform profiles for properties like temperature, salinity and momentum down to a specific depth: the mixed-layer depth. With this assumption, the turbulent kinetic energy (TKE) equation can be integrated over the mixed layer to find an expression for the change in TKE as a function of fluxes at the top and bottom of the mixed layer.

Our version of the bulk mixed-layer scheme, by Sterl and Kattenberg (1994), is developed for incorporation in an OGCM with fixed model levels and uses a slightly different approach. First the total amount of available TKE is computed that results from applying the surface fluxes to the surface layer. Next this amount of TKE is spent by mixing in deeper layers of the model, using the following equation

$$\Delta\mathrm{TKE} = s\Delta\mathrm{KE} + n\Delta\mathrm{PE} + \mathrm{WE}\,. \qquad (2.1)$$

Here ΔKE and ΔPE are the difference between the kinetic and potential energies of the water column before and after the adding of a deeper layer to the mixed layer. Whereas ΔKE is always positive, ΔPE is positive if an unstable stratification is removed (convection) and negative if dense water is mixed upward into the already-mixed layer (entrainment). When the contribution from these terms is positive, only a fraction s or n is added to the TKE budget. $(1 - s)$ and $(1 - n)$ are the fractions of the energy that are dissipated. In the case of ΔPE acting as a sink of TKE, n is set to 1. Following Niiler and Kraus (1977), we use $s = 0.7$ and $n = 0.2$.

The wind input in (2.1) is given by

$$\mathrm{WE} = mu_*^3 e^{-d/l_m}\Delta t\,. \qquad (2.2)$$

Here $u_* = \sqrt{|\vec{\tau}_0|/\rho_0}$ is the friction velocity in water, with $\vec{\tau}_0$ and ρ_0 the surface wind stress and the surface density of water, respectively. d is the depth. $l_m = m_2 u_*/f$ (with $m_2 = 0.4$, Oberhuber, 1993, and $f = 2\Omega\sin\phi$ the Coriolis parameter) is a length scale parameter and resembles the Ekman depth over which TKE from wind input is to decay exponentially. Δt is the time step and m is an empirical constant with a value of $m = 1.25$ according to Niiler and Kraus (1977). It represents the portion of available kinetic energy to the mixed layer from the wind. The exponential in (2.2) represents the dissipation of wind energy over a length scale typical to the Ekman depth. When there is insufficient TKE left to mix in yet another layer, the layer below the fully mixed layer is mixed in partially. The mixed-layer depth is determined as the depth at which all the TKE is spent.

A uniform layer implies efficient mixing at each time step, *i.e.*, immediate redistribution. This feature is fundamentally different from the nonlocal diffusion scheme, which specifically determines the diffusive characteristics of the boundary layer, as described in the next section.

2.2 The nonlocal diffusion scheme

The nonlocal diffusion scheme is based on the nonlocal K profile scheme from Large et al. (1994). This scheme is an adapted version of the nonlocal K profile scheme for the atmospheric boundary layer, which was developed by Troen and Mahrt (1986) and Holtslag and Boville (1993). The scheme is consistent with Monin-Obukhov similarity theory in the surface layer and incorporates the effect of countergradient fluxes for temperature and salinity.

At each step the scheme determines the boundary-layer depth h as the depth d for which a bulk Richardson number Ri_b exceeds a critical value Ri_c ($\mathrm{Ri}_c = 0.3$, Large et al., 1994):

$$\mathrm{Ri}_b(d) = \frac{\left(B_r - B(d)\right) d}{\left|\vec{V}_r - \vec{V}(d)\right|^2 + V_t^2(d)}\,. \qquad (2.3)$$

Here $B(d)$ and $V(d)$ are the instantaneous buoyancy and velocity profile of the water column. The subscript r denotes reference values near the surface. The denominator of (2.3) has a depth-dependent turbulent velocity shear $V_t(d)/d$ incorporated, associated

with the stochastic turbulent motions in the fluid. This term is important in convective situations with little or no mean shear. The turbulent velocity shear is parameterized following Large et al. (1994) as:

$$\frac{V_t^2(d)}{d^2} \propto \frac{Nw_s}{\mathrm{Ri}_c\, d} \tag{2.4}$$

The turbulent velocity shear is a function of the Brunt-Väisällä frequency N, the turbulent velocity scale w_s, the depth d, and the Richardson number Ri_c. The subscript s denotes the turbulent velocity scale for scalars. The functional form of the velocity scales w_x is different for momentum and scalars and follows from an empirical determination from measurements in the atmospheric boundary layer (Högström, 1988). In the formulation of Large et al. (1994), the properties of the turbulent velocity scale are chosen in a way that w_x is equal to u_* in neutral atmospheric forcing conditions and proportional to $w_* = (-hB_f)^{1/3}$ in highly unstable atmospheric forcing conditions. Here, $\kappa = 0.4$ is the Von Kármán constant and B_f is the buoyancy forcing. The constant of proportionality in (2.4) is set to give the correct ratio of the entrainment flux over the surface buoyancy flux in situations of pure convection, according to the empirical rule of convection, $\overline{wb}_e/\overline{wb}_0 = \beta_T$, with $\beta_T = -0.2$.

The turbulent flux of a property X in the boundary layer is formulated in terms of a diffusivity K_x and a nonlocal transport term γ_x, with subscript x referring to the property X:

$$\overline{wx}(d) = -K_x(\partial_z X - \gamma_x)\,. \tag{2.5}$$

The diffusivity is determined as a function of the mixed-layer depth h, the turbulent velocity scale $w_x(d)$, and a cubic polynomial in depth $G(\sigma)$, with $\sigma = d/h$ the dimensionless depth:

$$K_x = hw_x G\,. \tag{2.6}$$

$G(\sigma)$ is subject to the condition that K_x and its vertical gradient match the interior values at h and behaves according the similarity theory in the surface layer, in particular $G(0) = 0$. Conditions are often well approximated by $G(1) = \partial_\sigma G(1) = 0$, leading to the result $G(\sigma) \approx \sigma(1-\sigma)^2$.

The nonlocal transport term γ_x represents nonlocal influences on the mixing by turbulence due to large eddies and can be countergradient in nature, *i.e.*, transport acting against the local property gradient. This term is negligible in stable forcing conditions and is set to zero in these situations. In the absence of a satisfactory theory, the nonlocal transport term is neglected for the turbulent momentum flux. Large et al. (1994) use the following expression for the parameterization of the nonlocal transport term:

$$\gamma_x = C_s \frac{\overline{wx}_0}{w_x h} \tag{2.7}$$

The nonlocal transport term is computed from surface fluxes, the vertical velocity scale and the mixed-layer depth. Large et al. (1994) derive for $C_s = 6.3$ to make (2.7) comply with the parameterization of Mailhôt and Benoit (1982) in highly convective situations.

2.3 The original HOPE scheme

The original HOPE mixing scheme consists of a crude mixed-layer approach. It consists of the determination of a diagnostic mixed-layer depth set to the depth that is 0.5°C cooler than SST. Over the mixed-layer depth the vertical eddy viscosity and diffusivity coefficients are enhanced by a mixed-layer contribution $W_T = \eta^{k-1} W_{T,0}$ with k the layer index. In the 20-level HOPE model $W_{T,0} = 2 \cdot 10^{-3}\mathrm{m}^2/\mathrm{s}$ and $\eta = 0.4$. Below the mixed layer this term is set to zero.

3. Numerical implementation

The implementation depends on the specific needs of the mixed-layer scheme. In this section the main features of the mixed-layer schemes are discussed and the way how they are implemented in the HOPE OGCM. The main target was to implement fully functional mixed-layer schemes in HOPE, while leaving the original HOPE code as much intact as possible.

3.1 Mixed-layer schemes in HOPE

In this section we give a description of how the mixed-layer subroutines are embedded in the HOPE source code. For a complete description of the HOPE model we refer to the HOPE manual, Wolff et al. (1997).

After the initialization of the HOPE model in OCEINI, the main time stepping loop OCESTEP starts (see chapter 4, HOPE manual, Wolff et al. (1997). In OCESTEP several subroutines are called which perform a specific task. The first two subroutines are OCTHER and OCWIND. An important part of these routines is to force the ocean with prescribed fluxes. In OCTHER also the baroclinic pressure is computed, convective adjustment is applied and vertical eddy viscosity and diffusivity coefficients are calculated. In the following subroutines the various ocean fields are updated according to the new conditions.

The key features of the nonlocal diffusion (NLD) scheme are the determination of the mixed-layer depth and the computation of eddy viscosity and diffusivity coefficients over that depth. The latter are matched to the viscosity and diffusivity fields in the interior. Therefore, it would seem logical to call the NLD scheme right after the two forcing routines of HOPE. The profiles of the eddy viscosity and diffusivity derived from the NLD scheme could then be matched to the interior fields from OCTHER at the depth of the mixed layer.

However, a problem with the determination of the mixed-layer depth would arise. It is evident from equation (2.3) that for the determination of the mixed-layer depth near surface reference values are evaluated, so continuous profiles are preferred. In the case of surface cooling, convective adjustment in OCTHER will smooth the profiles for temperature and salinity to a certain extent, but in the case of surface heating the forcing part of OCTHER will leave a sharp jump between the first and the second layer. For the velocity profiles a jump will be left in either case. Hence, in order to prevent unphysical discontinuities in the buoyancy and velocity profiles interfering with the computation of the mixed-layer depth, it is necessary to precede the forcing by the determination of the mixed-layer depth, which leads to a separation in the mixed-layer scheme.

Also needed for the determination of the mixed-layer depth are the surface buoyancy forcing B_f and the friction velocity in water u_*, computed from the surface fluxes. Surface fluxes in the HOPE model not only consist of atmospheric fluxes, but also of flux corrections that depend on the actual ocean fields. In the original HOPE code the surface fluxes are computed and simultaneously applied to the ocean fields in OCTHER and OCWIND. Hence, in the case of the NLD scheme, it is also necessary to separate the computation of the surface fluxes from the forcing of OCTHER and OCWIND into a new subroutine called OCFLUX. In appendix B the code of this subroutine is shown together with the modifications to the two original forcing routines. In Figure 1 a graphical representation of the double separation of the subroutines is shown in the form of a flowchart.

For the bulk mixed-layer scheme this separation is not necessary. The entire mixing scheme can be called after the forcing routines, but for the sake of uniformity PREMIX is also called before the forcing routines. It might seem that mixing in the BML case occurs twice, because the vertical eddy viscosity and diffusivity coefficients are not set to zero in the mixed layer. But because properties over the depth of the mixed layer are supposed to be uniform after the BML scheme is called, vertical mixing by eddy coefficients will only have a small impact at the base of the mixed layer.

As mentioned, in OCTHER convective adjustment is applied. In a rather crude way convective adjustment removes unstable stratification by averaging temperature and salinity of the unstable layer with the underlying layer in a single sweep through the water column from top to bottom. In fact this is in a sense mixing by definition and it would be desirable to disable convective adjustment in conjunction with a sophisticated mixed-layer scheme. But in the case of the HOPE model the convective adjustment step is crucial for the computation of the initial viscosity and diffusivity profiles, because these depend on a stable stratification. With the proper adjustments to the code, it might be possible to correct for this problem. On the other hand the effects of this extra convective adjustment are not large, as it does not influence the depth of the mixed layer much. Within the mixed layer the BML scheme mixes everything anyway, whereas the NLD scheme would approximate this state fairly quickly.

The switch IMIXLAY determines which mixed-layer scheme is to be used: IMIXLAY = 1 and IMIXLAY = 2 results in the utilization of the NLD and the BML scheme respectively. IMIXLAY = 0

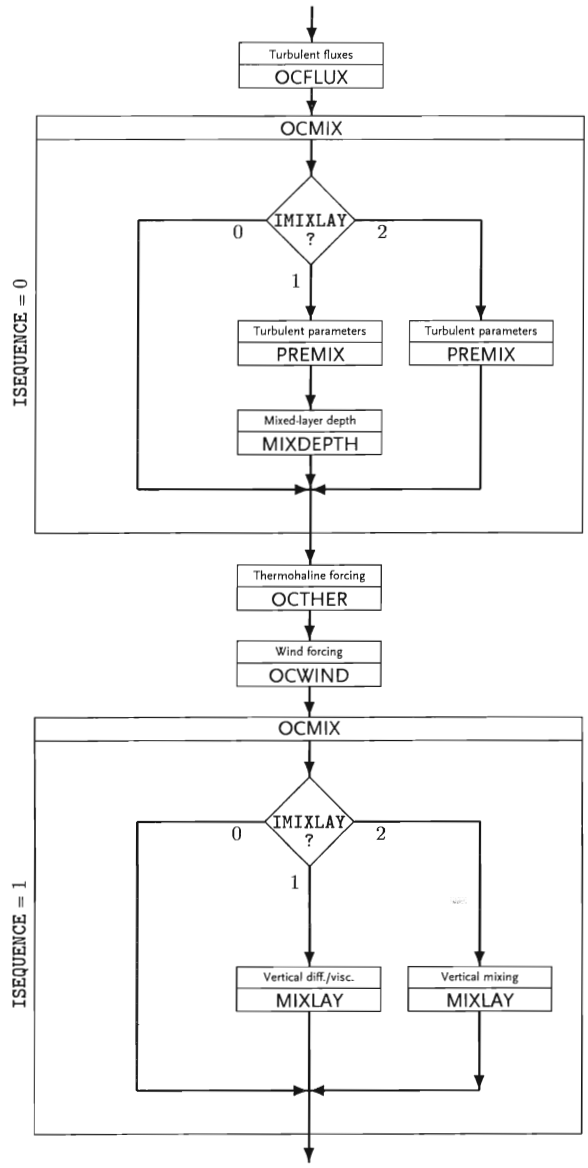

Figure 1: Flowchart of the implementation of the NLD/BML mixed-layer scheme.

results in the original HOPE mixing scheme and a null subroutine for OCMIX is called, which immediately returns to OCESTEP. For a proper representation of the physics, the parameter W_T has to be set to zero in the case IMIXLAY > 0.

In table 1 the modifications and additions to the original HOPE model source files, include files and namelists are listed.

3.2 The nonlocal diffusion scheme

The nonlocal diffusion scheme consists of six separate subroutines. The main subroutine OCMIX calls the routines: PREMIX, MIXDEPTH and MIXLAY. Additionally there are two service routines: VELOCITY and EXPCOEF. The structure of the code will be discussed in this section. For brevity only the 'even code' of the E-grid is shown. In the case of coupling terms between the even and odd grid the full code is given.

3.2.1 Calling conventions

The main subroutine OCMIX is called twice from OCSTEP, before OCTHER and after OCWIND. In each pass of OCMIX a different task has to be performed. In the first pass PREMIX and MIXDEPTH are called. PREMIX primarily computes the buoyancy forcing and the friction velocity and MIXDEPTH determines the mixed-layer depth. This has to be done before any forcing is applied to the surface, as discussed in the previous section. In the second pass MIXLAY is called. MIXLAY computes the profiles of the eddy viscosity and diffusivity in the mixed layer matched to interior profiles and applies the nonlocal forcing due to the countergradient terms to the temperature and salinity fields (see equation 2.6). In order to perform an identical subroutine call in OCESTEP for all values of IMIXLAY, the parameter ISEQUENCE is created, which can only have the value 0 or 1. In the first pass ISEQUENCE is set to zero and PREMIX and MIXDEPTH are called. In the second pass ISEQUENCE is set to 1, so MIXLAY is called. At the end of the calls ISEQUENCE flips to its counter value. In OCMIX:

```
IF (ISEQUENCE.EQ.0) THEN
  CALL PREMIX
  CALL MIXDEPTH(
#include ''dyn_outarg.h''
  )
ENDIF
IF (ISEQUENCE.EQ.1) THEN
  CALL MIXLAY
ENDIF
ISEQUENCE = 1-ISEQUENCE
```

In the header of the subroutine a special include file is to be inserted that only states some dynamical output arguments. This is a heritage from the original HOPE code.

3.2.2 The first pass

In the first pass OCMIX calls the subroutines PREMIX and MIXDEPTH. PREMIX starts with the initialization of the mixed-layer depth HBLE and the mixed-layer depth identifier KWUE, which identifies the deepest layer interface within the mixed layer.

Modification/addition	Remarks
add the files ocflux.F, mix.F, mixcom.h and mixpar1.h to the original HOPE source.	mix.F could be either the NLD scheme, the BML scheme or a null scheme. See appendix B for source of ocflux.F.
Modify ocbndr.F.	See appendix B for details.
`#include "mixcom.h"`	In beginning of OCEINI.
`NAMELIST/OCMIX/IMIXLAY`	In OCEINI after `NAMELIST/OCTIME/`.
`IMIXLAY = 1` `ISEQUENCE = 0`	In OCEINI after `ICONVA = 1`.
`READ (IOCTL, OCMIXS)`	In OCEINI after `READ(IOCTL,OCPHYS)`.
`IF (IMIXLAY.NE.0) WT=0`	In the beginning of section D of OCTHER.

`CALL OCMIX(`
`#include "dyn_outarg.h"`
`)`
	In OCESTEP before `CALL OCTHER` and the second time after `CALL OCWIND`.

`CALL OCFLUX`	in OCESTEP before first call of OCMIX.

`&OCMIXS`
`IMIXLAY = $IMIXSCHEME`
`&OCMIXS`
	In the file ocectl after namelist "OCPHYS". $IMIXSCHEME is a shell variable from the submitted job used to run HOPE.

Table 1 The complete set of modifications and additions to the original HOPE source code required for the implementation of the NLD or the BML scheme. See Figure 1 for a flowchart of the implementation.

The initialization is only done in the first time step, defined by the logical FIRST. In PREMIX

```
IF (FIRST) THEN
  DO J=1,JE
    DO I=1,IE
      KWUE(I,J) = 1
      HBLE(I,J) = 0.0
    ENDDO
  ENDDO
ENDIF
```

The next step is to compute the buoyancy profiles BE. For this computation the thermal expansion coefficients of the density, ALTE and ALSE, are required. They are calculated in the service routine EXPCOEF.

```
CALL EXPCOEF(THE,SAE,PREFF,ALTE,ALSE)
DO K=1,KE
  DO J=1,JE
    DO I=1,IE
      BE(I,J,K) = G*(ALTE(I,J,K)*THE(I,J,K)
                - ALSE(I,J,K)*SAE(I,J,K))
    ENDDO
  ENDDO
ENDDO
```

The last step in PREMIX computes the buoyancy forcing BFE and the friction velocity in water USTARE. The buoyancy forcing is made up by two contributions: a turbulent part WBTURE and a non-turbulent part WBRADE. The turbulent part is simply computed from the surface fluxes from OCFLUX for temperature and salinity, WTHE and WSAE, using the thermal expansion coefficient of the density from EXPCOEF. The non-turbulent part is the integral over the depth of the mixed layer of the solar radiation, which is used for the heating of the mixed layer. Solar radiation passing through the mixed layer does not contribute to the buoyancy forcing. The friction velocity in water is directly computed from the surface fluxes of the longitudinal and meridional velocities, WUKE and WVKE, also from OCFLUX.

```
DO J=1,JE
  DO I=1,IE
    WBRADE = 0.0
    DO K=1,KE
      FLAGE  = 0.5 - SIGN(0.5,KWUE(I,J)-K)
      WBRADE = WBRADE
             + G*ALTE(I,J,K)*WJE(I,J,K)*FLAGE
    ENDDO
    KWE = KWUE(I,J)
    WBRADE = WBRADE
           + G*WJE(I,J,KWE)*ALTE(I,J,KWE)
             *(HBLE(I,J)-TIESTW(KWE))/DZW(KWE)
    WBTURE = G*(ALTE(I,J,1)*WTHE(I,J)
           - ALSE(I,J,1)*WSAE(I,J))
    BFE(I,J)    = -WBTURE - WBRADE
    USTARE(I,J) = SQRT(SQRT(WUKE(I,J)**2
                + WVKE(I,J)**2))
  ENDDO
ENDDO
```

After PREMIX, MIXDEPTH is called which determines the mixed-layer depth from buoyancy and velocity profiles, when the bulk Richardson number RIE exceeds a certain critical value. Because the mixed-layer depth is determined on P points, auxiliary velocity fields on P points have to be computed from the original velocity fields. This computation is straightforward, considering an E-grid. With the auxiliary velocity fields available now, the Richardson

numbers are computed according to (2.3). It is worth noting that the computation of the mixed-layer depth and therefore also the computation of the Richardson number is performed on layer interfaces. The fields of buoyancy and velocity therefore have to be averaged on W-levels. For the turbulent shear term (2.4) the turbulent velocity scale WS, and the Brunt-Väisällä frequency XNE are required. The turbulent velocity scales for scalars and momentum are calculated in the service routine VELOCITY. The Brunt-Väisällä frequency is calculated from the STABIE array, which is a measure for the vertical stability of the water column. In this formulation of the bulk Richardson number the buoyancy and velocity at depth are evaluated against near surface reference values. This depth HREF is one fourth of the first layer thickness and reference values are equivalent to the first elements of the buoyancy and velocity profiles. In MIXDEPTH

```
DO K=2,KE
  HNEW = TIESTW(K)
  HREF = 0.5*TIESTU(1)
  DO J=1,JE
    DO I=1,IE
      HDEPTH(I,J) = HNEW
      SIGMA(I,J)  = 1.0
    ENDDO
  ENDDO
  CALL VELOCITY(SIGMA,HDEPTH,USTARE,BFE,WAE,
                                          WDE)
  DO J=1,JE
    DO I=1,IE
      BEAVG  = 0.5*(BE (I,J,K)+BE (I,J,K-1))
      UEDAVG = 0.5*(UED(I,J,K)+UED(I,J,K-1))
      VEDAVG = 0.5*(VED(I,J,K)+VED(I,J,K-1))
      XNE    = SQRT(MAX(G*STABIE(I,J,K),0.0))
      VT2E   = CV/RIC/XKAPPA**2
               *SQRT(-BETAT/CS/EPSSUR)
               *HNEW*XNE*WDE(I,J) + EPPS
      RIE(I,J,K) = MAX(0.0,
               (BE(I,J,1)-BEAVG)*(HNEW-HREF)/
               (VT2E + (UED(I,J,1)-UEDAVG)**2
               + (VED(I,J,1)-VEDAVG)**2))
    ENDDO
  ENDDO
ENDDO
```

Before the actual determination of the mixed-layer depth can start a few boundary conditions and limitations have to be set. First the boundary values of the Richardson number are set to 0 at the surface (TIESTW(1)) and to the critical Richardson number Ri_c at the base of the deepest layer (TIESTW(KEP)). In this way the mixed-layer depth will not be identical to zero in the case of open water, and will never exceed the theoretical bottom of the model in absence of topography. Next the mixed-layer depth and mixed-layer identifier as well as the factor of the next layer to be added to the mixed layer, FACTORE, are initialized. Finally supplementary boundaries for the mixed-layer depth are computed. First a maximum mixed-layer depth HBLEMAX is imposed, in this version this is set to 250 m. This empirical limit is to prevent extreme mixed-layer depths which cause unrealistic convection. Second a minimum mixed-layer depth HBLEMIN is computed, which is a function of the depth of the first grid point, the maximum mixed-layer depth and a depth determined by the braking of surface waves, Burgers (1996).

```
DO J=1,JE
  DO I=1,IE
    RIE(I,J,1)   = 0.0
    RIE(I,J,KEP) = RIC
    KWUE(I,J)    = 1
    HBLE(I,J)    = 0.0
    FACTORE(I,J) = 1.0
    HBLEMAX(I,J) = MIN(DEPTE(I,J),250.)
    HBLEMIN(I,J) = MAX(DDPE(I,J,1)/2.,
                       5.0E5*USTARE(I,J)**2/G)
    HBLEMIN(I,J) = MIN(HBLEMIN(I,J),
                       HBLEMAX(I,J))
  ENDDO
ENDDO
```

Now the determination of the mixed-layer depth can commence. This scheme evaluates at every W-level the conditions for the critical Richardson number and the minimum or maximum mixed-layer depth, and sets the associated flag to 0 if fulfilled and to 1 if not. The associated fraction which is to be added to the so far determined mixed layer according to the specific condition is 1 for an unfulfilled condition (*i.e.*, an entire layer is to be added) and less than 1 for a fulfilled condition. The combined flag FLAGE ultimately determines what fraction FLAGFACE is to be added to mixed layer. Once FLAGE is set to 0 the mixed layer will stay unaltered.

```
DO K = 2,KEP
  HNEW = TIESTW(K)
  DNEW = DZW(K-1)
  DO J=1,JE
    DO I=1,IE
      FLAGHNE  = 0.5 - SIGN(0.5,
                            HNEW-HBLEMIN(I,J))
      FACHNE   = (HBLEMIN(I,J)-HNEW)/DNEW+1.
      FLAGHME  = 0.5 - SIGN(0.5,
                            HNEW-HBLEMAX(I,J))
      FACHME   = (HBLEMAX(I,J)-HNEW)/DNEW+1.
      FLAGRIE  = 0.5 - SIGN(0.5,
                            RIE(I,J,K)-RIC)
      FACRIE   = (RIC-RIE(I,J,K-1))
                 /ABS(RIE(I,J,K)-RIE(I,J,K-1)
                      + EPPS)
      FLAGE    = MAX(FLAGHME*FLAGRIE,FLAGHNE)
      FLAGFACE = MAX(FACHNE,FLAGHME*FACRIE
                 + FLAGRIE*FACHME
                 + (1-FLAGRIE)*(1-FLAGHME)
                   *MIN(FACRIE,FACHME))
      FACTORE(I,J) = INT(FACTORE(I,J))
                 *(FLAGE + (1-FLAGE)*FLAGFACE)
```

```
      KWUE(I,J) = KWUE(I,J)+INT(FACTORE(I,J))
      HBLE(I,J) = HBLE(I,J)+DNEW*FACTORE(I,J)
    ENDDO
  ENDDO
ENDDO
```

Finally the global mixed-layer depth fields are written to output using the subroutine OUTPROC. This completes the first pass of OCMIX.

3.2.3 The second pass

The second pass of OCMIX is after OCTHER and OCWIND have been applied. In this pass MIXLAY is called. MIXLAY computes the eddy viscosity and diffusivity profiles in the mixed layer. They are matched to the interior profiles from OCTHER at the depth of the mixed layer, determined in MIXDEPTH. The interior profiles are simply overwritten by the new profiles above the mixed-layer depth. As for the velocity profiles in MIXDEPTH the interior profiles of the eddy viscosity are to be averaged on P points. For the computation of the profiles the coefficients of the third degree polynomial ($G(\sigma)$ in equation (2.6)) have to be calculated from the matching constraint. For a elaborate discussion of this procedure we refer to Large et al. (1994). For this procedure the following parameters at the depth of the mixed layer are required: the turbulent velocity scales for momentum and scalars, WAE and WDE, and their vertical derivatives, WAZE and WDZE; the values of the viscosity and diffusivity, AV1E and DV1E, and their vertical derivatives, AV1ZE and DV1ZE; and from the former parameters the value of the polynomial for viscosity and diffusivity, GA1E and GD1E, and their vertical derivatives, GA1ZE and GD1ZE. D1E and D2E are corrected layer thicknesses near the bottom of the ocean. In the routine MIXLAY this is coded as

```
CALL VELOCITY(SIGMAE,HBLE,USTARE,BFE,WAE,WDE)
DO J=1,JE
  DO I=1,IE
    KWE = KWUE(I,J)
    K1 = MIN(KWE+1,KEP)
    K2 = MIN(KWE+2,KEP)
    D1E   = MAX(MIN(DEPTE(I,J)-TIESTW(KWE),
                DZW(MIN(KWE,KE))),EPPS)
    D2E   = MAX(MIN(DEPTE(I,J)-TIESTW(K1),
                DZW(MIN(KWE+1,KE))),EPPS)
    RRE   = (HBLE(I,J)-TIESTW(KWE))
            /DZW(MIN(KWE,KE))*D2E
            /DZW(MIN(KWE+1,KE))
    AV1ZE = MAX(ADE(I,J,KWE)-ADE(I,J,K1),0.)
            *(1-RRE)/D1E
          + MAX(ADE(I,J,K1) - ADE(I,J,K2),0.)
            *RRE/D2E
    DV1ZE = MAX(DVE(I,J,KWE) - DVE(I,J,K1),0.)
            *(1-RRE)/D1E
          + MAX(DVE(I,J,K1) - DVE(I,J,K2),0.)
            *RRE/D2E
    AV1E  = ADE(I,J,K1)
          + AV1ZE*(TIESTW(KWE)+D1E-HBLE(I,J))
    DV1E  = DVE(I,J,K1)
          + DV1ZE*(TIESTW(KWE)+D1E-HBLE(I,J))
    WAZE  = -5.*HBLE(I,J)*BFE(I,J)*WAE(I,J)**2
            /(USTARE(I,J)**4+EPPS)
            *(1+SIGN(1.,BFE(I,J)))/2.
    WDZE  = -5.*HBLE(I,J)*BFE(I,J)*WDE(I,J)**2
            /(USTARE(I,J)**4+EPPS)
            *(1+SIGN(1.,BFE(I,J)))/2.
    GA1E(I,J) = AV1E/(HBLE(I,J)*WAE(I,J)+EPPS)
    GD1E(I,J) = DV1E/(HBLE(I,J)*WDE(I,J)+EPPS)
    GA1ZE(I,J) = MIN(-AV1ZE/WAE(I,J)-GA1E(I,J)
                     *WAZE/WAE(I,J),0.)
    GD1ZE(I,J) = MIN(-DV1ZE/WDE(I,J)-GD1E(I,J)
                     *WDZE/WDE(I,J),0.)
  ENDDO
ENDDO
```

With the coefficients of the polynomial $G(\sigma)$ computed, the entire profile in the mixed layer of the eddy viscosity and diffusivity can be determined according to equation (2.6). Also the nonlocal transport terms are computed. For convenience they are multiplied by the diffusivity, resulting in GKTE = $K_s\gamma_\theta$ for temperature and GKSE = $K_s\gamma_\theta$ for salinity. K_s stands for the vertical eddy diffusivity coefficient for scalars and the subscripts θ and s in the nonlocal transport term γ stand for temperature and salinity. A flag, set to zero for positive buoyancy forcing is, included in the nonlocal terms. After the computation of the profiles of viscosity, a back transition has to be done to vector points on an E-grid.

```
DO K=1,KEP
  HDEPTH = TIESTW(K)
  DO J=1,JE
    DO I=1,IE
      SIGMAE(I,J) = HDEPTH/(HBLE(I,J)+EPPS)
    ENDDO
  ENDDO
  CALL VELOCITY(SIGMAE,HBLE,USTARE,BFE,WAE,
                                          WDE)
  DO J=1,JE
    DO I=1,IE
      GAE = SIGMAE(I,J)*(1.-SIGMAE(I,J))**2
          + GA1E(I,J) *SIGMAE(I,J)**2
            *(3.-2.*SIGMAE(I,J))
          + GA1ZE(I,J)*SIGMAE(I,J)**2
            *(SIGMAE(I,J)-1.)
      GDE = SIGMAE(I,J)*(1.-SIGMAE(I,J))**2
          + GD1E(I,J) *SIGMAE(I,J)**2
            *(3.-2.*SIGMAE(I,J))
          + GD1ZE(I,J)*SIGMAE(I,J)**2
            *(SIGMAE(I,J)-1.)
      FLAGBFE = 0.5 - SIGN(0.5,BFE(I,J))
      FLAGHME = 0.5 + SIGN(0.5,KWUE(I,J)-K)
      GKTE(I,J,K) = FLAGHME*FLAGBFE*CCS
                    *(WTHE(I,J)+WJE(I,J,1))*GDE
      GKSE(I,J,K) = FLAGHME*FLAGBFE*CCS
                    *WSAE(I,J)*GDE
```

```
      ADE(I,J,K) = MIN((1-FLAGHME)*ADE(I,J,K)
                 +    FLAGHME*HBLE(I,J)
                     *WAE(I,J)*GAE,0.5)
      DVE(I,J,K) = MIN((1-FLAGHME)*DVE(I,J,K)
                 +    FLAGHME*HBLE(I,J)
                     *WDE(I,J)*GDE,0.5)
    ENDDO
  ENDDO
ENDDO
```

The final step is to apply the nonlocal transport applied to the temperature and salinity fields.

```
DO K=1,KE
  DZWI = 1./DZW(K)
  DO J=1,JE
    DO I=1,IE
      THE(I,J,K) = THE(I,J,K)+DT*DZWI
                  *(GKTE(I,J,K+1)-GKTE(I,J,K))
      SAE(I,J,K) = SAE(I,J,K)+DT*DZWI
                  *(GKSE(I,J,K+1)-GKSE(I,J,K))
    ENDDO
  ENDDO
ENDDO
```

The service routine VELOCITY computes the turbulent velocity scales for momentum and scalars, WM and WS, from the ratio of the depth to the mixed layer SIGMA, the depth HH, the friction velocity in water USTAR, and the buoyancy forcing BF. For an elaborate discussion of functional form of the velocity scales, we refer to Large et al. (1994). It is coded as

```
DUM(XDUM) = 0.5+SIGN(0.5,XDUM)
DO J=1,JE
  DO I=1,IE
    SIGMAX = MIN(SIGMA(I,J),
          (1+EPSSUR+SIGN(1-EPSSUR,BF(I,J)))/2)
    ZZ = SIGMAX*HH(I,J)*XKAPPA*BF(I,J)
         /(USTAR(I,J)+EPZ)**3
    PHIM = DUM(ZZ) *(1+5*ZZ)
         + DUM(ZZ-ZM)*(1-DUM(ZZ))
                  *(1-16*MIN(ZZ,0.))**(-1./4.)
         + (1-DUM(ZZ-ZM))
                 *(BM-CM*MIN(ZZ,ZM))**(-1./3.)
    PHIS = DUM(ZZ) *(1 +5*ZZ)
         + DUM(ZZ-ZS)*(1-DUM(ZZ))
                  *(1-16*MIN(ZZ,0.))**(-1./2.)
         + (1-DUM(ZZ-ZS))
                 *(BS-CS*MIN(ZZ,ZS))**(-1./3.)
    WM(I,J) = XKAPPA*(USTAR(I,J)+EPZ)/PHIM
    WS(I,J) = XKAPPA*(USTAR(I,J)+EPZ)/PHIS
  ENDDO
ENDDO
```

The service routine EXPCOEF computes the thermal expansion coefficients of the density. The density is computed from a simplified version of the UNESCO formula from Gill (1982). The thermal expansion coefficients then are found taking the T-derivative for temperature and the S-derivative for salinity. The main part is

```
DO K=1,KE
  P = PIN(K)
  DO J=1,JE
    DO I=1,IE
      T = TIN(I,J,K)
      S = SIN(I,J,K)
      R = A00 + S*A01
        + T*(A10 + S*A11 + T*(A20 + T*A30))
        + P*(B00 + T*(B10 + T*B20) + S*B01
             + P*(C00+T*C10+P*D00))
      ALTIN(I,J,K) = -(A10 + S*A11
                   + T*(2.*A20+3.*T*A30)
                   + P*(B10+2.*T*B20+P*C10))/R
      ALSIN(I,J,K) =  (A01 + T*A11 + P*B01)/R
    ENDDO
  ENDDO
ENDDO
```

3.3 The bulk mixed-layer scheme

The bulk mixed-layer scheme consists of three separate subroutines. The main subroutine OCMIX calls the routines: PREMIX and MIXLAY. The relative small number of subroutines and the simplicity of the BML scheme as compared to the NLD scheme make this scheme faster. The structure of the code will be discussed in this section.

The main subroutine OCMIX in the case of the BML scheme is also called twice from OCSTEP. In the first pass only PREMIX is called, analogous to the NLD scheme, and primarily computes the friction velocity. In the second pass MIXLAY is called which determines the mixed-layer depth and mixes the water column actively. This version of OCMIX is

```
IF (ISEQUENCE.EQ.0) THEN
  CALL PREMIX
ENDIF
IF (ISEQUENCE.EQ.1) THEN
  CALL MIXLAY(
#include "dyn_outarg.h"
  )
ENDIF
ISEQUENCE = 1-ISEQUENCE
```

PREMIX starts with the initialization of the mixed-layer depth HBLE and the mixed-layer depth identifier KWUE, identical to the NLD scheme. The only remaining action of PREMIX then is to compute the friction velocity in water also as with the NLD scheme.

In the second pass MIXLAY is called, which determines the mixed-layer depth and simultaneously mixes the water column up to that depth. Again the mixed-layer depth is determined on P points, therefore auxiliary velocity fields on P points, UED and VED, have to be calculated from the original velocity fields. In addition to this procedure averaged velocity fields over the depth of the mixed layer are computed, UMIXE and VMIXE. The auxiliary velocity fields

then are premixed over this depth to ensure the conservation of momentum. In MIXLAY this is coded as

```
DO K=1,KE
  DO J=2,JE1
    DO I=2,IE1
      KWE = MAX(KWUE(I,J),2)
      FLAGE = 0.5 + SIGN(0.5,KWE-1-K)
      UED(I,J,K) = (1-FLAGE)*UED(I,J,K)
                 + FLAGE*UMIXE(I,J)
      VED(I,J,K) = (1-FLAGE)*VED(I,J,K)
                 + FLAGE*VMIXE(I,J)
    ENDDO
  ENDDO
ENDDO
```

Before the actual mixing can start a few boundary conditions and limitations have to be set. First the mixed-layer depth and mixed-layer identifier as well as the factor of the next layer to be added to the mixed layer, FACTORE, are initialized. This initialization is identical for the NLD scheme. The supplementary boundaries for the mixed-layer depth are slightly different in the case of the BML scheme. The maximum mixed-layer depth HBLEMAX is simply equal to the bottom topography. There is no need for an additional hard depth limitation. The minimum mixed-layer depth HBLEMIN is computed, as in the NLD scheme. Because mixed-layer determination and mixing are performed simultaneously, the averaged fields for temperature TMIXE and salinity SMIXE have to be initialized. They are set to the value of the first layer. Also the initial budget of the turbulent kinetic energy TKEE is to be calculated. This is simply the wind input at the surface from equation (2.2). Finally the inverse of the Ekman depth, DECAYE, is computed.

```
DO J=1,JE
  DO I=1,IE
    KWUE(I,J)    = 1
    HBLE(I,J)    = 0.0
    FACTORE(I,J) = 1.0
    HBLEMAX(I,J) = DEPTE(I,J)
    HBLEMIN(I,J) = MAX(DDPE(I,J,1)/2.,
                       5.0E5*USTARE(I,J)**2/G)
    HBLEMIN(I,J) = MIN(HBLEMIN(I,J),
                       HBLEMAX(I,J))
    TMIXE(I,J)   = THE(I,J,1)
    SMIXE(I,J)   = SAE(I,J,1)
    TKEE(I,J)    = DT*EMM*USTARE(I,J)**3
    DECAYE(I,J) = ABS(F(2*J  )
                  /(DECMUL*USTARE(I,J)+EPPS))
    DECAYO(I,J) = ABS(F(2*J-1)
                  /(DECMUL*USTARO(I,J)+EPPS))
  ENDDO
ENDDO
```

For the determination of the mixed-layer depth the same procedure with flags and fractions is used as with the NLD scheme. Instead of the computation of a bulk Richardson number, here mixing in a deeper layer causes a change in the TKE budget. If the total TKE budget is spent, again a flag is set to zero and the associated fraction of the next layer is added to the mixed-layer depth. A change in the TKE budget, DIFTKEE, is caused by three factors, see equation (2.1): a change in potential energy, DIFPE, or kinetic energy, DIFKE, and dissipation of wind energy, DIFWE. For the exact formulations of these terms we refer to Sterl and Kattenberg (1994). For the computation of the change in potential energy the density is required. This is computed with the UNESCO formula for the density, Gill (1982), also used by HOPE. In this version of the BML scheme the change in kinetic energy is not considered, because of numerical stability problems with this term. Sterl and Kattenberg (1994), also decided to discard this term, because they found that the contribution of the term, if taken into account, is minor compared to the other terms in (2.1). After every update of the mixed-layer depth and its identifier, the mixed-layer temperature, salinity, zonal and meridional velocities are computed by simply averaging over the yet determined mixed-layer depth. When the TKE budget is spent, the underlying layer is partially mixed with the mixed layer.

```
DO K = 2,KEP
  HOLD = TIESTW(K-1)
  HNEW = TIESTW(K)
  DNEW = DZW(K-1)
  DO J=1,JE
    DO I=1,IE
      SHELP(I,J)=SAE(I,J,K-1)
      THELP(I,J)=THE(I,J,K-1)
    ENDDO
  ENDDO
  CALL RHO1(THELP,SHELP,PREFF(K-1),RHOE)
  CALL RHO1(TMIXE,SMIXE,PREFF(K-1),RMIXE)

  DO J=1,JE
    DO I=1,IE
      FLAGHNE = 0.5 - SIGN(0.5,
                           HNEW-HBLEMIN(I,J))
      FACHNE  = (HBLEMIN(I,J)-HNEW)/DNEW+1.
      FLAGHME = 0.5 - SIGN(0.5,
                           HNEW-HBLEMAX(I,J))
      FACHME  = (HBLEMAX(I,J)-HNEW)/DNEW+1.
      WINDE = DT*EMM*USTARE(I,J)**3
              *EXP(-DECAYE(I,J)*HOLD)
      DIFWE = WINDE*(EXP(-DECAYE(I,J)*DNEW)-1)
      DIFPE = 0.5*G*(HNEW-DNEW)*DNEW
              *(1-RHOE(I,J)/(RMIXE(I,J)+EPPS))
      DIFKE = 0.5*(1-DNEW/HNEW)*DNEW
              *((UED(I,J,K-1)-UMIXE(I,J))**2
               +(VED(I,J,K-1)-VMIXE(I,J))**2)
      DIFTKEE = DIFWE
              + DIFPE*(1-DISP*(0.5+SIGN(0.5,
                                        DIFPE)))
Commented out + DIFKE*(1-DISK)
      TKEE(I,J)= TKEE(I,J) + DIFTKEE
      FLAGTKE  = 0.5 + SIGN(0.5,TKEE(I,J) +
```

```
                    0.5*G*HOLD*DNEW*1E-6)
      FACTKE    = MAX((TKEE(I,J)-DIFTKEE)
                     /ABS(-DIFTKEE+EPPS),0.0)
      FLAGE     = MAX(FLAGHME*FLAGTKE,FLAGHNE)
      FLAGFACE  = MAX(FACHNE,FLAGHME*FACTKE
                  + FLAGTKE*FACHME
                  + (1-FLAGTKE)*(1-FLAGHME)
                    *MIN(FACTKE,FACHME))
      FACTORE(I,J) = INT(FACTORE(I,J))*(FLAGE
                       + (1-FLAGE)*FLAGFACE)
      SFACTORE = 1.-SQRT(1.-FACTORE(I,J))
      KWUE(I,J) = KWUE(I,J)
                + INT(FACTORE(I,J))
      HBLE(I,J) = HBLE(I,J) + FACTORE(I,J)
                            *(HNEW-HBLE(I,J))
      UMIXE(I,J) = UMIXE(I,J) + SFACTORE
                  *(UED(I,J,K-1)-UMIXE(I,J))
                  *DNEW/HNEW
      VMIXE(I,J) = VMIXE(I,J) + SFACTORE
                  *(VED(I,J,K-1)-VMIXE(I,J))
                  *DNEW/HNEW
      TMIXE(I,J) = TMIXE(I,J) + FACTORE(I,J)
                  *(THE(I,J,K-1)-TMIXE(I,J))
                  *DNEW/HNEW
      SMIXE(I,J) = SMIXE(I,J) + FACTORE(I,J)
                  *(SAE(I,J,K-1)-SMIXE(I,J))
                  *DNEW/HNEW
      THE(I,J,K-1) = THE(I,J,K-1)
                  - FACTORE(I,J)*(1-FLAGE)
                   *(THE(I,J,K-1)-TMIXE(I,J))
                   *HOLD/HNEW
      SAE(I,J,K-1) = SAE(I,J,K-1)
                  - FACTORE(I,J)*(1.-FLAGE)
                   *(SAE(I,J,K-1)-SMIXE(I,J))
                   *HOLD/HNEW
      UED(I,J,K-1) = UED(I,J,K-1)
                  - SFACTORE*(1-FLAGE)
                   *(UED(I,J,K-1)-UMIXE(I,J))
                   *HOLD/HNEW
      VED(I,J,K-1) = VED(I,J,K-1)
                  - SFACTORE*(1-FLAGE)
                   *(VED(I,J,K-1)-VMIXE(I,J))
                   *HOLD/HNEW
    ENDDO
  ENDDO
ENDDO
```

The next step is to implement the computed values for the mixed layer into the ocean fields. A flag is designed to determine which fields have to be replaced. The final step of this routine is to translate the computed fields of the velocity on P-points back the vector points (not shown).

```
DO K=1,KE
  DO J=1,JE
    DO I=1,IE
      FLAGE = 0.5 - SIGN(0.5,K-KWUE(I,J))
      THE(I,J,K) = FLAGE*TMIXE(I,J)
                 + (1-FLAGE)*THE(I,J,K)
      SAE(I,J,K) = FLAGE*SMIXE(I,J)
                 + (1-FLAGE)*SAE(I,J,K)
      UED(I,J,K) = FLAGE*UMIXE(I,J)
                 + (1-FLAGE)*UED(I,J,K)
      VED(I,J,K) = FLAGE*VMIXE(I,J)
                 + (1-FLAGE)*VED(I,J,K)
    ENDDO
  ENDDO
ENDDO
```

4. Some results

In this section we describe a set of three experiments with the mixed layer schemes, implemented in the h2e4 version of the HOPE model run at the European Centre for Medium Range Forecasts (ECMWF). First, a control run with the original HOPE mixing scheme. Second, a run with the NLD scheme, and third, a run with the BML scheme implementation.

The HOPE model is run over a period of nine years, starting from the first of January 1986. Most of the evaluation will be made on the basis of the final year of the runs to avoid complications with spin-up effects. Global SST and surface salinity fields will be investigated with respect to observed fields. Also, a closer look will be taken at the thermocline structure in the equatorial Pacific. Finally, the existence of barrier layers in the NLD run will be shown.

4.1 Model initialization and forcing

In all cases, the initial condition of the model is prescribed by a restart file from a previous run of the HOPE model with the original mixing scheme. The forcing is prescribed using daily ERA fluxes for the years 1986–1993. From 1994 on, fluxes are used from operational data. Also, a restoring heat flux to observed SST (Reynolds and Smith, 1994) of 15 $W/m^2 K$ is applied to the surface. Surface salinity is relaxed globally to observed monthly fields from Levitus (1982). In polar regions salinity and temperature below ice is also relaxed, using a pseudo ice model, which prescribes the monthly amount of ice cover.

4.2 Surface fields

Figures 2–3 show the bias of the global SST fields to observed fields (Reynolds and Smith, 1994) during the northern winter and the northern summer of 1994. In the northern winter season the first striking difference in comparing the three runs is the apparent absence of an overestimation of SST by more than 2°C in the southern Arctic Ocean in the BML run, compared to the control and the NLD run. Less prominent in size, but equally significant, is the absence of a cold anomaly in the mid-equatorial Pacific in the BML run. A similar feature of the three runs is the large bias in the Atlantic Ocean, particularly in the region of the Gulf Stream.

In Figure 4 (top) the zonally averaged root-mean-squared (RMS) error of the SST fields compared to observed is displayed for the northern winter season. Also noted from this picture, the difference between the runs in the southern Arctic Ocean is the most prominent. The BML scheme displays a RMS error that is about 1.5°C lower than the other runs. The figure also shows the smaller bias of the BML scheme in the Atlantic Ocean around

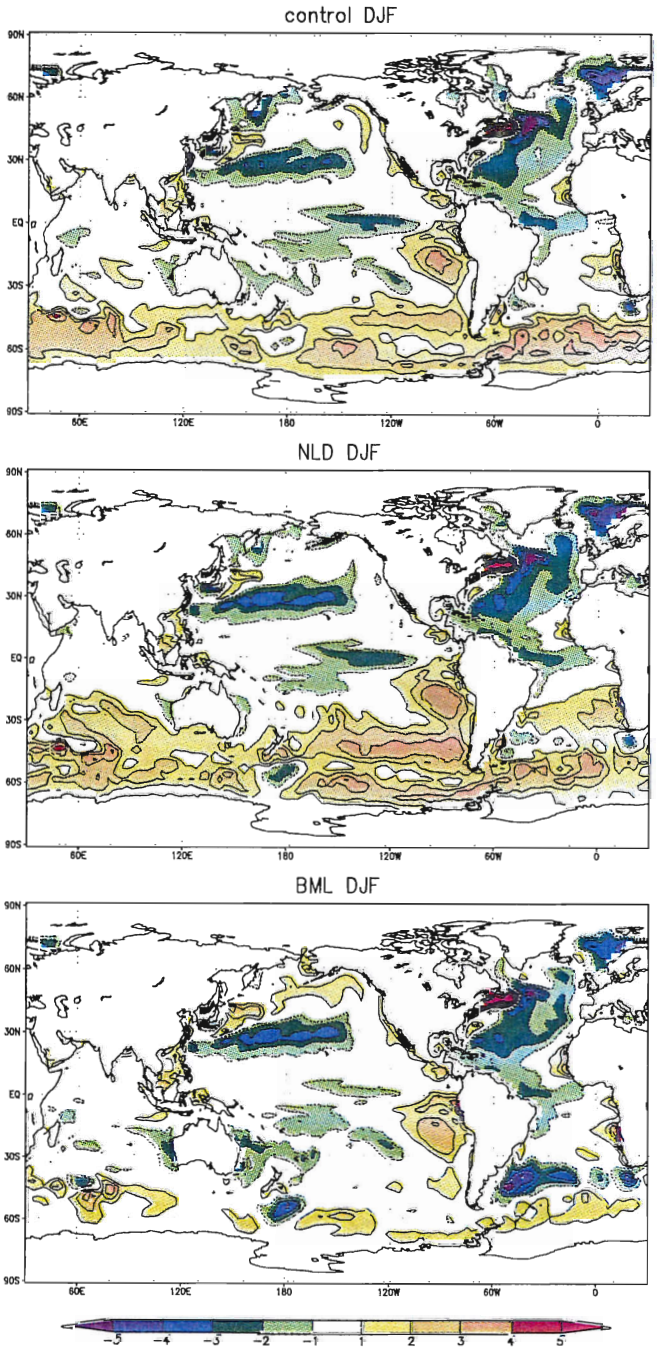

Figure 2: SST bias with respect to observed fields during the northern winter in the control run (top), NLD scheme (middle) and BML scheme (bottom).

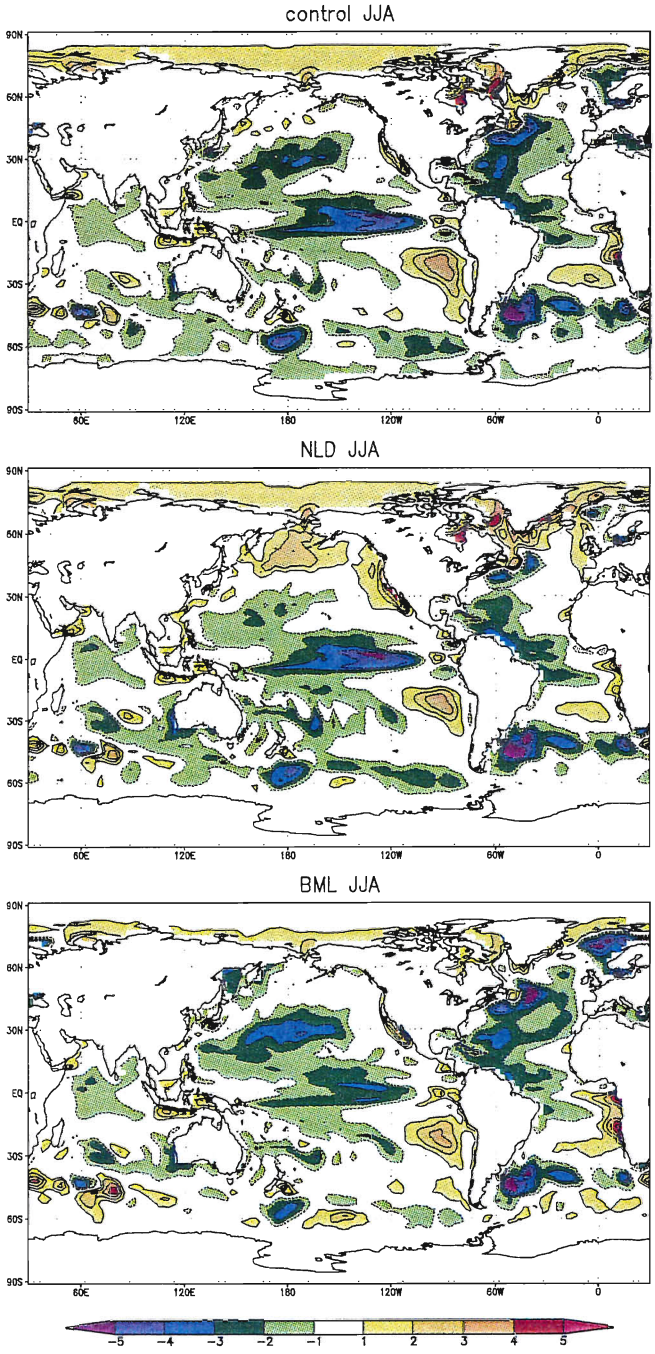

Figure 3: SST bias with respect to observed fields during the northern summer in the control run (top), NLD scheme (middle) and BML scheme (bottom).

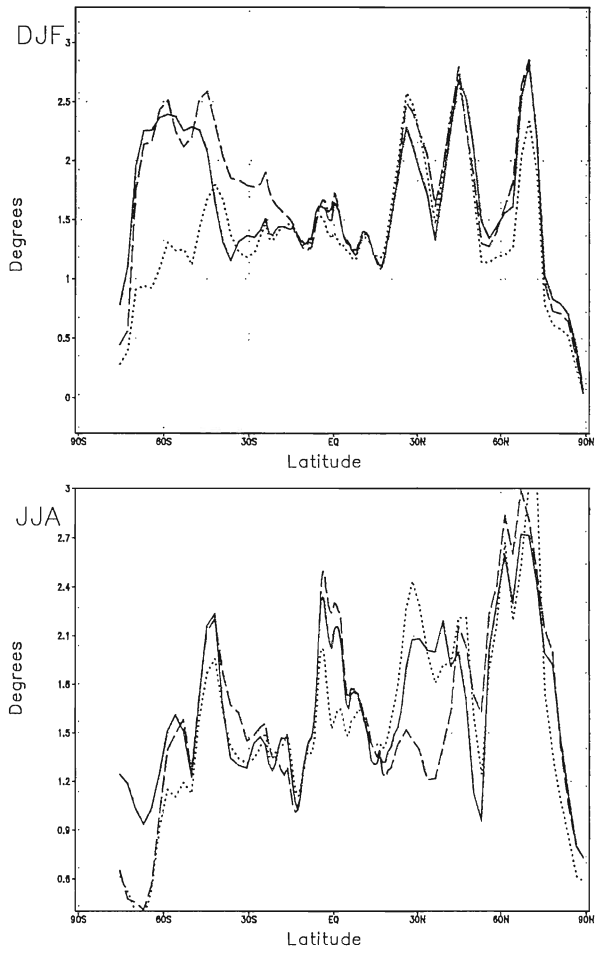

Figure 4: Top: RMS error of the zonally averaged SST fields with respect to observations during the northern winter for the control run (solid), the NLD run (dashed) and the BML run (dotted). Bottom: same, but for the northern summer.

60°N, by half a degree. Zonally averaged, the disappearance of the cold equatorial anomaly in the BML run is compensated by positive anomalies elsewhere to give equal results as the other runs in the tropical region. The NLD run shows a rather high RMS error around the southern mid-latitudes.

From Figure 5, which displays the mixed-layer depths for the three runs during the northern winter, we can make an effort to explain some of the features described above. For Figure 5 the mixed-layer depth is computed according to the half-degree difference with SST criterion, because the definition 'mixed-layer depth' is not the same in all schemes and therefore direct comparison is not possible. From Figure 5, all runs display deep mixed layers in the extreme southern Arctic Ocean. North of 60°S, the three runs differ. In the summer there is a clear coupling between mixed-layer depth and SST in this region: a shallower mixed layer distributes the heat flux over less water, giving a higher SST. The warm bias in the top and middle panels of Figure 2 can therefore be explained by the very shallow mixed-layer depth in the control run and NLD model. The BML scheme generates a mixed-layer depth of 60–100 m, leading to an almost correct representation of the SST.

In the tropical region the situation is often reversed: a shallow mixed layer in an upwelling region indicates the presence of cold water near the surface, giving rise to lower SST. The reduction of the cold bias in the central tropical Pacific in the BML scheme can be seen to correspond with deeper mixed layers in this region. In the northern subtropics these deeper layers again give a cold bias.

For the northern mid-latitudes similar patterns for mixed-layer depth exist in all runs. A deep mixed layer in the area of deep water formation. For the BML run the deep mixed layers seem to be extended further to the south. Again the NLD model gives results very similar to the original HOPE scheme.

During the northern summer (Figure 2) the anomalies in the southern Arctic Ocean of the BML scheme are smaller compared to the control run, now in the order of 1°C (see Figure 43 bottom). The NLD run wanders between the other two. Differences are less pronounced because at the Southern Hemisphere it is wintertime and mixed layers are deep everywhere (not shown). Around the equator there are clear differences between the runs. For SST the BML scheme performs better and the RMS error is reduced by almost 1°C. Also the NLD scheme does a better job, although the improvement in RMS error is much less. In the northern mid-latitudes the NLD run shows better results for the RMS error whereas the BML is somewhat worse than the control run.

In Figure 6 a global picture of the surface salinity fields, compared to the control run, is displayed. In the absence of comprehensive data sets of salinity fields no comparison with observations is made here and only some differences with the original run are pointed out. One of the most evident features of Figure 6 is the ability of the BML and the NLD scheme to generate a larger amplitude in

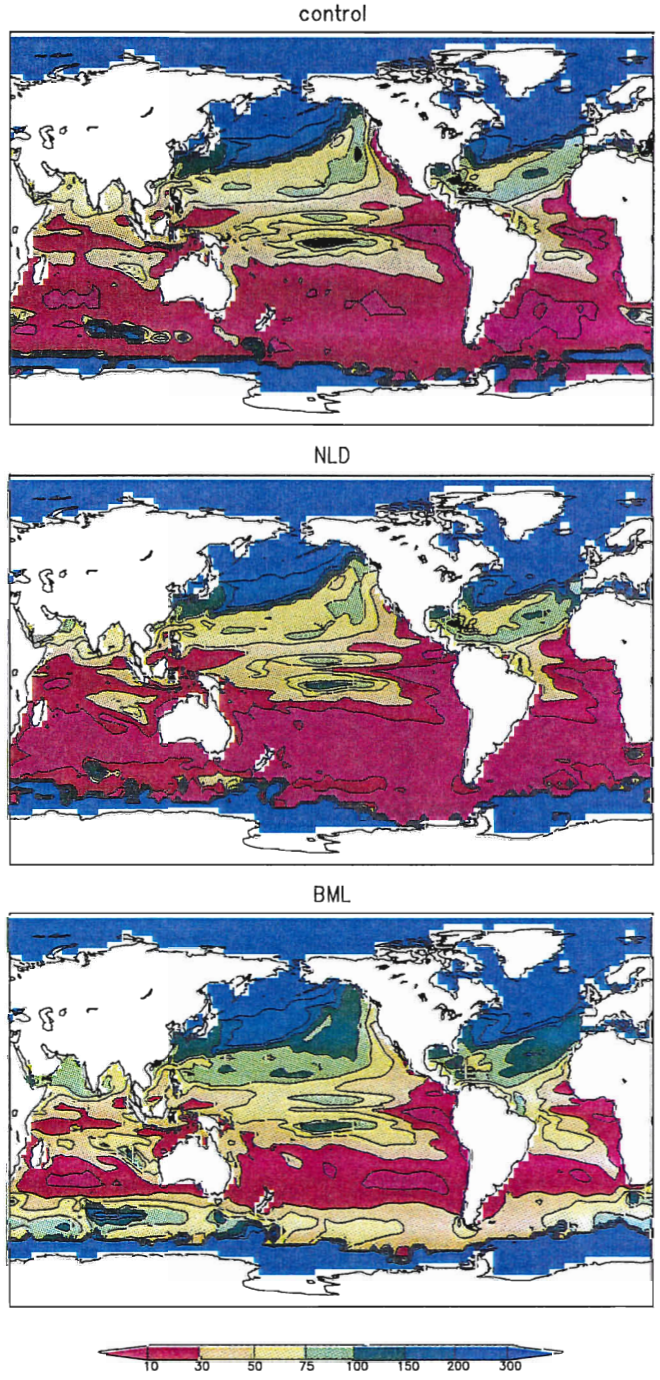

Figure 5: The mixed-layer depth according to half-degree difference with SST criterion for the control run (top), the NLD run (middle) and the BML run (bottom) for the winter months of 1994

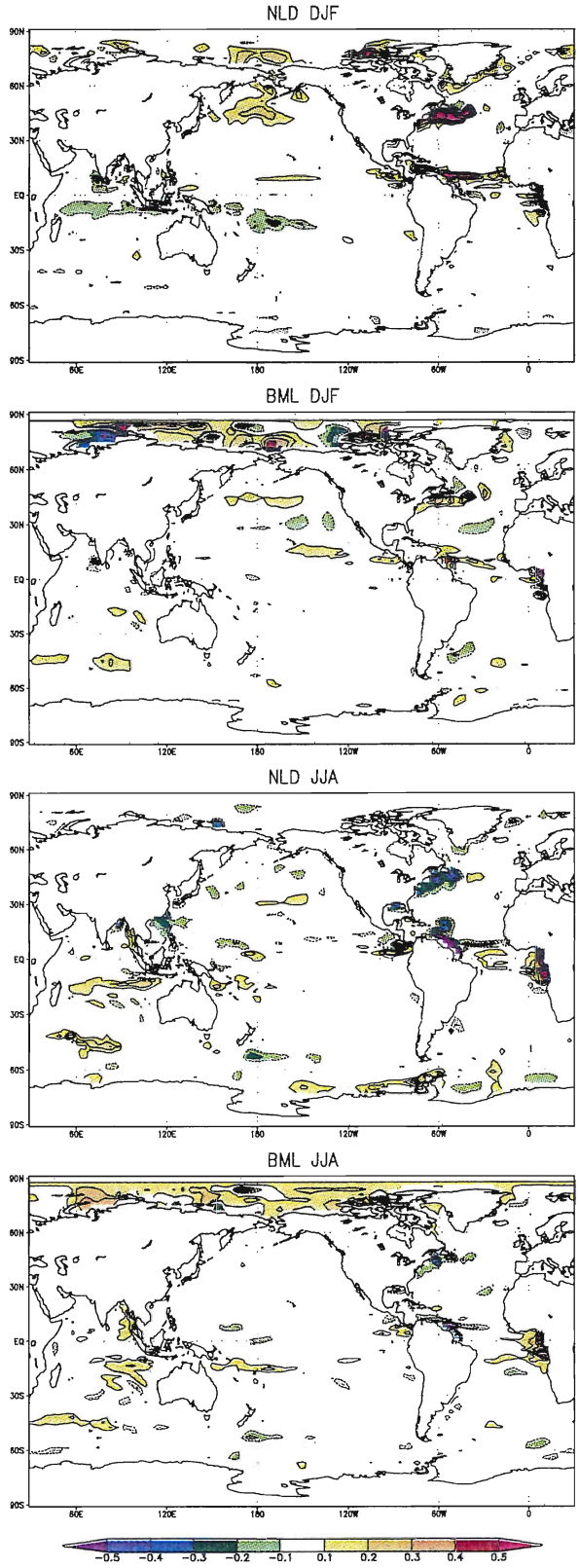

Figure 6: The top two figures show the sea surface salinity anomalies with respect to the control run during the northern winter for the NLD run and the BML run. The bottom two figures show the same for the northern summer.

the annual signal of the surface salinity in particular areas. For example in the Gulf Stream region, for both mixed-layer schemes the water is more saline in the winter and more fresh in the summer. The consequences of the different salinity patterns in this region could have effect on the deep water formation, but is not investigated and beyond the scope of this document. The BML run also shows some distinct differences in the northern Arctic ocean compared to the control run.

4.3 Thermocline structure

Figure 7a shows the observed thermocline structure of the Pacific Ocean from 140°E–95°W to a depth of 500 m, for the month of August 1994, averaged from 2°S–2°N, derived from analyzed fields (mainly TOGA/TAO array data, assimilated into the same HOPE model). Easy to identify in this figure is the Warm Pool as the blob of 29°C warm water in the top left section. Also evident is the sharp thermocline, shoaling from around 200 m in de west Pacific to less than 50 m in the eastern side of the basin.

In Figures 7b,c,d the results for the HOPE model are displayed, for respectively, the control, the NLD and the BML run, in similar fashion as Figure 7a. In first order the model resembles the observed thermocline structure well. The thermocline has a comparable shoaling and is equally sharply defined. The warm pool in the west Pacific has comparable depth and temperature, but the eastern edge seems to be shifted somewhat to the west. In fact, as shown in the previous section (see Figure 2), the entire surface fields along the equatorial Pacific displays rather large anomalies during the northern summer. In Figures 7b,c,d the cold anomalies are identified as the 'outcropping' of the isotherms too far to the west. From Figure 7a we see that over the displayed domain the 21°C isotherm does not surface. For the control and the NLD run the amount of outcrop is rather similar, but both show outcropping up to the 19°C isotherm. The BML scheme has a much more true to nature upper thermocline structure and the first outcrop involves the 21°C isotherm.

Below the thermocline, the structure for all runs is similar, apart from the extreme eastern side of the basin. In this region the HOPE model displays a peculiar structure, giving rise to an unstable temperature stratification. Off course, taken into account the effects of salinity (also displayed in Figure 7 as the open contour field) on the density, the water column is stable. A similar structure is evident in the NLD run, although the 14°C isotherm follows a slightly different path. On the other hand the BML scheme limits the formation of an unstable temperature stratification in this region.

The salinity fields from the three runs are almost identical, except for the upper ocean structure in the Warm Pool. The control run and the BML run display a homogeneous profile for temperature and salinity up to a comparable depth of around 50 m, whereas the NLD shows a similar depth for the temperature profile, but for salinity the homogeneity is limited to the first 25 m.

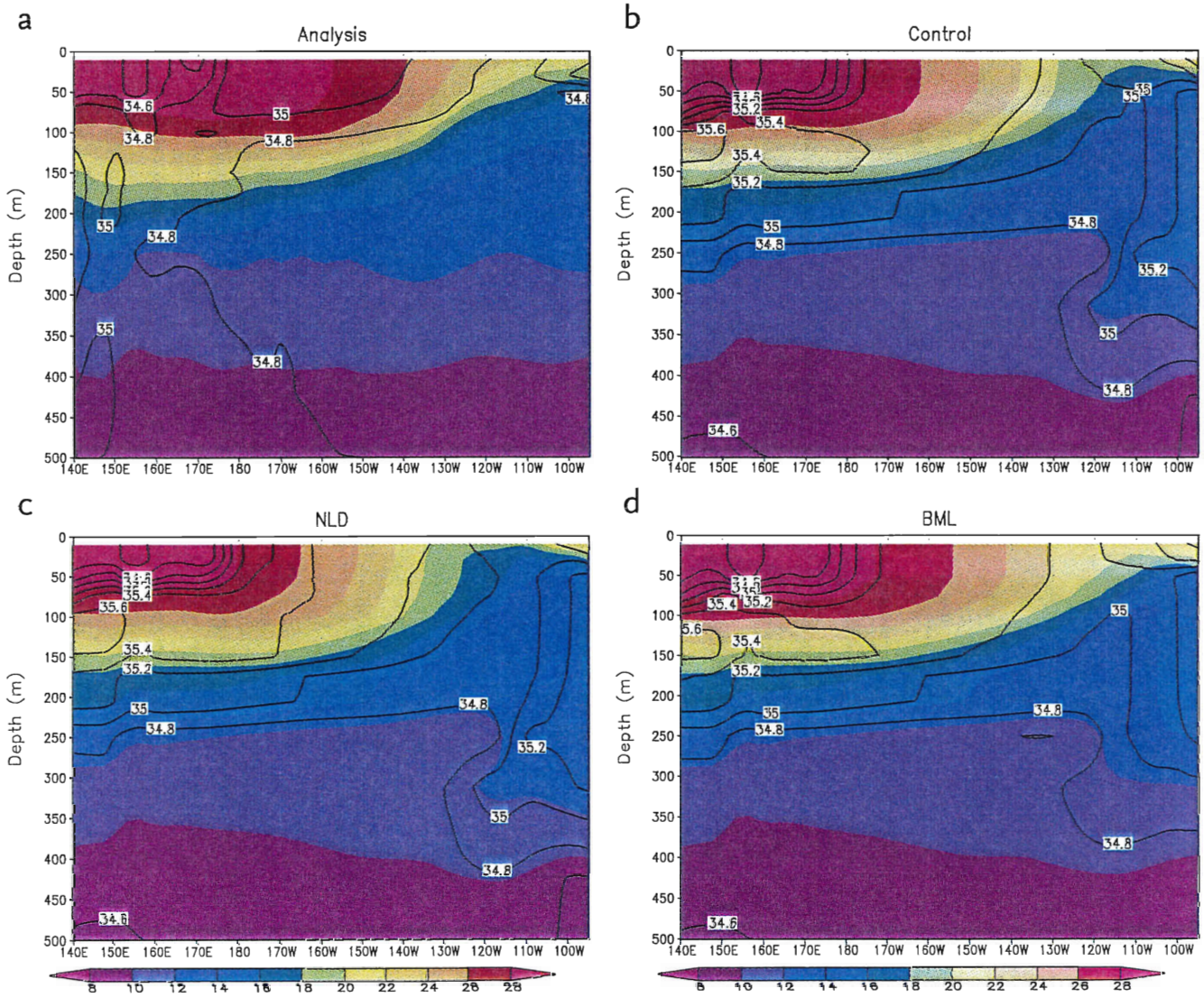

Figure 7: The thermocline structure of the Pacific Ocean to a depth of 500 m, for the month of August 1994, averaged from 2° S-2° N, (a) from an analysis with TOGA/TAO data assimilation, (b) the control run, (c) the NLD run and (d) the BML run. The shaded contours display the temperature and the open contour the salinity fields.

Also the 35.4 PSU isohaline shows an outcrop at the surface. This difference in depths of homogeneity is associated with the formation of barrier layers. In the next section particular profiles from the runs will be evaluated against an observed profile, to have a closer look at the identification of a barrier layer as a robust feature of the NLD scheme.

Figure 8 shows a cross section at 0.25°S for the zonal velocity component. Unlike the thermocline structure, for the zonal velocity the BML run displays a remarkable resemblance with the control run. Only a slight difference of around 0.10 m/s is visible in the surface current. The core velocity is respectively 0.97 m/s and 0.95 m/s. In the case of the NLD scheme the strength of the undercurrent seems to be diminished over a large extent of the thermocline and the core velocity has dropped considerable to 0.83 m/s. For all runs the core undercurrent is located at 0.25°S, *i.e.*, the model latitude closest to the equator. The results for the strength of the undercurrent differ substantially from observations. The average core velocity at this location is approximately 1.21 m/s (CTD database NOAA PMEL, Ando and McPhaden, 1997).

4.4 The barrier layer

Figure 9a shows observed profiles for temperature and salinity, on 21 March 1993 14:58 hr at 4°S 164°E (CTD database NOAA PMEL, Ando and McPhaden, 1997). The mixed layer is identified as approximately the upper 80 m of the water column, where temperature and salinity are more or less homogeneous distributed. If considering the simple half-degree temperature difference with SST criterion, one can identify an even deeper isothermal layer, up to a depth of more than 100 m. The layer below the mixed layer until the isothermal layer depth, is called the barrier layer, marked by near neutral temperature stratification and sharp vertical salinity gradients. Barrier layers are formed at times of heavy precipitation and by subduction of the denser saline water masses during advection. Barrier layers are common in the western equatorial Pacific, Ando and McPhaden (1997).

In Figure 9b the model results for the three runs are displayed, approximately at the same time and location. The profiles are from a single grid point on 3.75°S 164°E, on 00:00 hr, March 21 1993. Although SST resembles the observation quite well, the surface salinity deviates by 0.4 PSU in every model run. This might be due to high temporal fluctuation in advection by sudden wind gusts or heavy precipitation, which could never be resolved in the HOPE model. Apart from this, it is a known issue that salinity is not well represented in the HOPE model, because of the uncertainty in the forcing and relaxation.

The depth of the isothermal layer for all model runs does substantially diverge from observations. The clear homogeneous layer is restricted to the upper 50 m, although, with the half-degree criterion, the isothermal layer could be extended to 75 m for the BML scheme. A similar depth applies for the salinity, except for the NLD scheme. Although the depth of the halocline

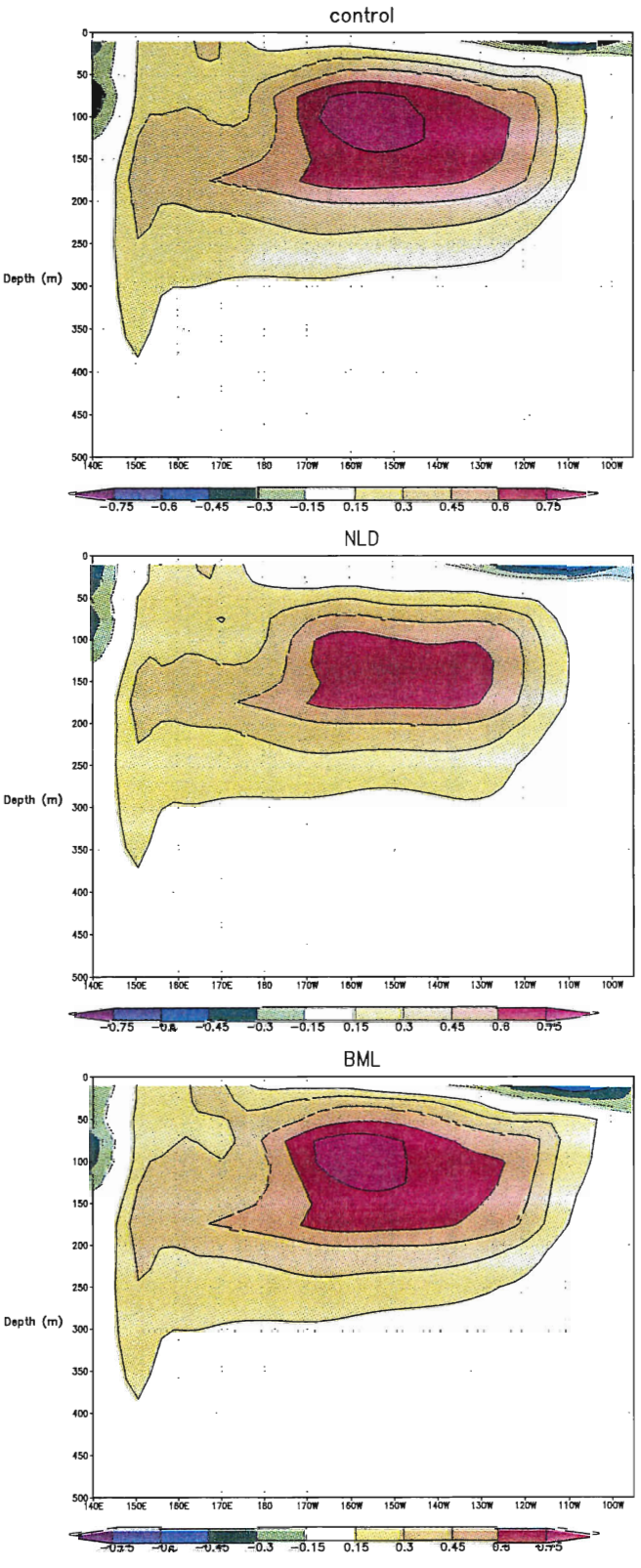

Figure 8: Zonal cross section at 0.25° S from 140° E - 95° W to a depth of 500m of the zonal velocity component, for the control run (top), the NLD run (middle) and the BML run (bottom) in August, 1994.

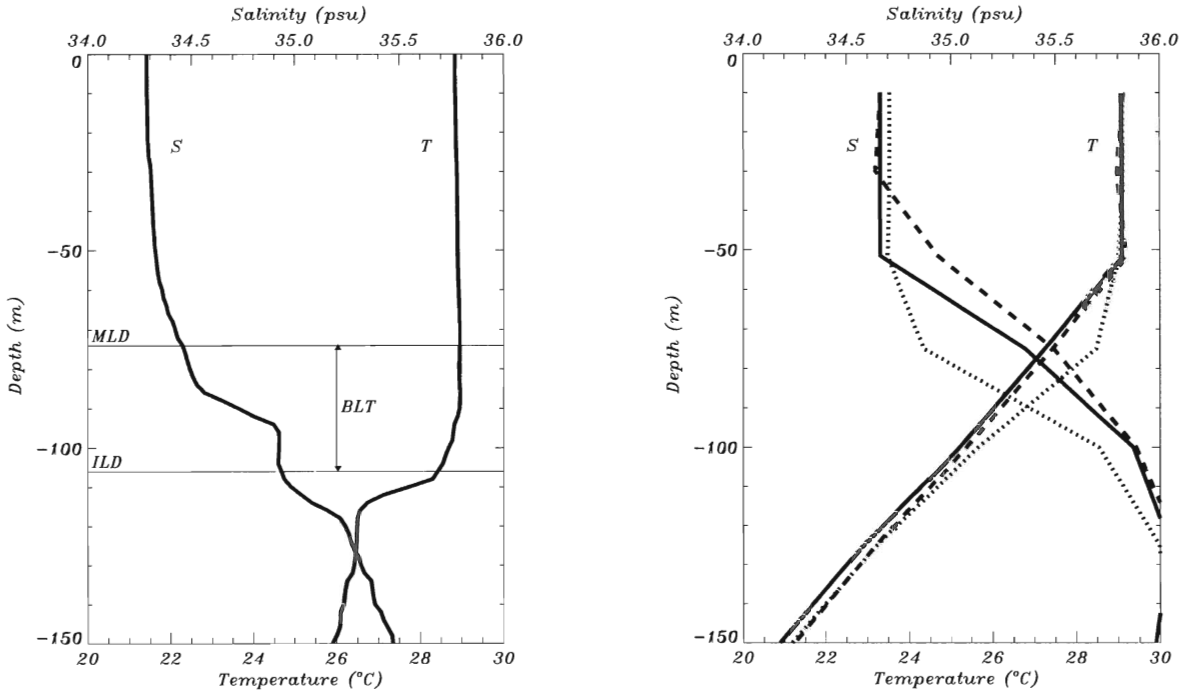

Figure 9: (a) Observed profiles for temperature and salinity, on 21 March 1993 14:58 hr at 4° S 164° E to a depth of 150 m. The isothermal layer depth (ILD) and mixed-layer depth (MLD) are identified as the depth to where, respectively, the temperature and temperature as well as salinity are homogeneous. The difference between these depths is the barrier layer thickness (BLT). (b) The profiles for temperature and salinity from the control run (solid), the NLD run (dashed) and the BML run (dotted), on 21 March 1993 00:00 hr at 3.75° S 164° E.

does not resemble the observed accurately, it is evident that the NLD scheme is capable of forming a distinct barrier layer with a thickness of 25 m, which is quite close to the thickness found in the observations. The outcrop of the 35.4 PSU isohaline, mentioned in the previous section, could point to the subduction of saline surface water as the possible cause of the formation of the barrier layer.

From a more comprehensive analysis of the model output, it was found that the formation of barrier layers is a robust feature of the NLD scheme.

4.5 Discussion

The implementation of two sophisticated mixed-layer schemes, a nonlocal diffusion (NLD) scheme and a bulk mixed-layer (BML) scheme, is very easy to accomplish, following the 'recipe' described in this document. Apart from a separation of the computation of the surface flux fields from the actual ocean forcing, the mixed-layer schemes behave like a plug-in to the HOPE model. The desired scheme, the original HOPE mixing scheme included, can be selected by setting a simple switch.

The BML scheme shows significant improvements in the global SST fields and equatorial thermocline structure. The NLD scheme is capable of producing barrier layers, which is a common observed feature in the western equatorial Pacific. By their concept of mixing, barrier layers cannot be formed with the original mixing scheme of the HOPE model or the BML scheme.

Coupled runs combined with the NLD scheme in a more recent version of the HOPE model by M. A. Balmaseda at the ECMWF, show even better results. In this experiment the maximum depth of the mixed layer ($HBL_{E/O}MAX$) was set to 60 m, instead of the 250 m used for the experiments in this document. In view of our results with the BML model with respects to the improvements to the global temperature fields, we recommend to also test this scheme in coupled run experiments.

Although in most OGCMs the vertical resolution in the upper ocean tends to be higher than in the deep ocean, the resolution still is too coarse to resolve the detailed mixed-layer processes. It is expected, strong improvements will be made with higher resolutions in the upper ocean, especially with the NLD scheme, because it is limited to a maximum mixed-layer depth and it is capable of resolving more detail in the profiles of temperature, salinity and velocity in the mixed layer, van Eijk et al. (1997). This is a important feature of the NLD scheme which is absent in any bulk mixed-layer scheme, including the BML scheme described in this document.

Computational costs increase by 12% and 30%, for the BML and NLD scheme, respectively, when the HOPE model is run on a

Fujitsu vpp700 at the ECMWF.

The final choice of a mixed-layer scheme between the BML and the NLD scheme, is one of a fast scheme, able to produce improved SST fields or a 'more complete' physical model, which is able to produce a feature like barrier layers. Resolution will play a major role in this decision. Therefore, we recommend the BML scheme when the vertical resolution is limited. In the case of high vertical resolution, the NLD scheme is preferred, especially if one has a particular interest in detailed mixed-layer processes.

Bibliography

Ando, K. and McPhaden, M. J. (1997): Variability of surface layer hydrography in the tropical Pacific Ocean. *J. Geophys. Res.*, **102**, 23063–23078.

Burgers, G. (1996): Comments on "Estimates of kinetic energy dissipation under breaking waves". *J. Phys. Oceanogr.*, **27**, 2306–2307.

Eijk, M. van, Burgers, G. and Holtslag, A. A. M (1997): An evaluation of two mixed-layer models. *KNMI preprint* 97–01.

Large, W. G., McWilliams, J. C. and Doney, S. C. (1994): Oceanic vertical mixing: A review and a model with a nonlocal boundary-layer parameterization. *Rev. Geophys.*, **32**, 363–403.

Levitus, S. (1982): Climatological atlas of the World Ocean. US Department of Commerce, NOAA Prof. Pap. 13.

Gill, A. E., (1982): *Atmosphere-Ocean Dynamics*. Academic Press, 662 pp.

Högström, U. (1988): Non-dimensional wind and temperature profiles in the atmospheric surface layer. *Bound.-Layer Meteor.*, **42**, 55–78.

Holtslag, A. A. M. and Boville, B. A. (1993): Local versus nonlocal boundary-layer diffusion in a global climate model, *J. Clim.*, **6**, 1825–1842.

Mailhôt, J. and Benoit, R. (1982): A finite-element model of the atmospheric boundary layer suitable for use with numerical weather prediction models. *Bound.-Layer Meteor.*, **60**, 143–168.

Mellor, G. L. and Yamada, T. (1982): Development of a turbulence closure model for geophysical fluid problems. *Rev. Geophys.*, **20**, 851–875.

Niiler, P. P. and Kraus, E. B. (1977): One dimensional models of the upper ocean. In: *Modeling and prediction of the upper layers of the ocean*, E. B. Kraus, ed., Pergamon Press, 143–177.

Oberhuber, J. M. (1993): Simulation of the Atlantic Circulation with a coupled sea ice-mixed-layer-isopycnal general circulation model, I: model description. *J. Phys. Oceanogr.*, **23**, 808–829.

Reynolds, R. W. and Smith, T. M. (1994): Improved global sea surface analyses using optimum interpolation. *J. Clim.*, **7**, 929–948.

Sterl, A. and Kattenberg, A. (1994): Embedding a mixed-layer model into an ocean general circulation model of the Atlantic: the importance of surface mixing for heat and temperature. *J. Geophys. Res.*, **99**, 14139–14157.

Troen, I. and Mahrt, L. (1986): A simple model of the atmospheric boundary layer; Sensitivity to surface evaporation. *Bound.-Layer Meteor.*, **37**, 129–148.

Wolff, J-O, Maier-Reimer, E. and Legutke, S. (1997): The Hamburg Ocean Primitive Equation Model. Technical Report No. 13, Deutsches Klimarechenzentrum, Hamburg. ISSN 0940-9327.

Appendix A
List of variables

This appendix deals with the parameters, constants and variables of the two mixed-layer schemes, that are not present in the original HOPE model. Each is sorted in several sections in analogue of the HOPE manual, Wolff et al. (1997). Every entry is described as local or global and is marked as a typical NLD and/or BML scheme. For common HOPE parameters, constants or fields, we refer to the HOPE manual, Wolff et al. (1997).

Table 2: Switches

Switch	Value	Description	Type	N	B
IMIXLAY	0	Null mixed-layer scheme	global	y	y
	1	NLD mixed-layer scheme			
	2	BML mixed-layer scheme			
ISEQUENCE	0	First OCMIX pass in OCESTEP	global	y	y
	1	Second OCMIX pass in OCESTEP			

Table 3: Model constants

Name	Symbol	Value	Description	Type	N	B
BETAT	T	-0.2	Ratio of entrainment flux and surface buoyancy flux	global	y	n
BM	c_m	8.38	Constant in stability functions ϕ_m, ϕ_s	global	y	n
BS	a_s	-28.86	Constant in stability functions ϕ_m, ϕ_s	global	y	n
CM	a_m	1.26	Constant in stability functions ϕ_m, ϕ_s	global	y	n
CS	c_s	98.96	Constant in stability functions ϕ_m, ϕ_s	global	y	n
CSTAR	C^*	10.0	Proportionality coefficient parameterizing s	global	y	n
CV	C_v	1.6	Ratio of Brunt-Väisällä frequencies in the mixed layer and at the entrainment depth	global	y	n
DECMUL	m_2	0.4	Constant in the Ekman length scale, see Niiler and Kraus (1977)	global	n	y
DISK	$1 - s$	0.3	Fraction of dissipated kinetic energy	global	n	y
DISP	$1 - n$	0.8	Fraction of dissipated potential energy	global	n	y
EMM	m	1.25	Constant in the wind input, see Niiler and Kraus (1977)	global	n	y
EPPSUR	ϵ	0.1	Nondimensional extent of the surface layer	global	y	n
EPZ	ϵ_z	10^{-12}	Small number used in VELOCITY	local	y	n
RIC	Ri_c	0.3	Critical Richardson Number	global	y	n
XKAPPA	κ	0.4	Von Kármán constant	global	y	n
ZM	ζ_m	-0.20	Constant in stability functions ϕ_m, ϕ_s	global	y	n
ZS	ζ_s	-1.0	Constant in stability functions ϕ_m, ϕ_s	global	y	n

Table 4: Model variables (3-D, dimension: IE, JE, KE+1)

Name	Symbol	Units	Description	Type	N	B
$\mathrm{GKS}_{E/O}$	$K_s\gamma_\theta$	PSU m/s	Nonlocal transport term for salinity, multiplied by the diffusivity coefficient for scalars	global	y	n
$\mathrm{GKT}_{E/O}$	$K_s\gamma_\theta$	Km/s	Same for temperature	global	y	n
$\mathrm{RI}_{E/O}$	Ri		Richardson number	local	y	n

Table 5: Model variables (3-D, dimension IE, JE, KE)

Name	Symbol	Units	Description	Type	N	B
$\mathrm{ALS}_{E/O}$	β	PSU^{-1}	Expansion coefficient for salt	local	y	n
ALSIN	β	PSU^{-1}	Aux. array for expansion coefficient for salt in EXPCOEF	local	y	n
$\mathrm{ALT}_{E/O}$	α	K^{-1}	Thermal expansion coefficient	local	y	n

ALTIN	α	K^{-1}	Aux. array for thermal expansion coefficient in EXPCOEF	local	y	n
$B_{E/O}$	B	m/s^2	Buoyancy	global	y	n
SIN	S	PSU	Auxiliary array for salinity in EXPCOEF	local	y	n
TIN	T	°C	Auxiliary array for temperature in EXPCOEF	local	y	n
$U_{E/O}D$	U	m/s	Auxiliary array for zonal velocity on scalar points	local	y	y
$V_{E/O}D$	V	m/s	Auxiliary array for meridional velocity on scalar points	local	y	y
$WJ_{E/O}$	J	Km/s	Non-turbulent temperature forcing from solar radiation	global	y	y

Table 6: Model variables (2-D, dimension IE, JE)

Name	Symbol	Units	Description	Type	N	B
$AD_{E/O}$	A_V	m^2/s	Aux. array for eddy viscosity on scalar points	local	y	n
$BF_{E/O}$	B_f	m^2/s^3	Surface buoyancy forcing	global	y	n
$DECAY_{E/O}$	l_m	m	Ekman length scale	local	n	y
$FACTOR_{E/O}$	f		Fraction of the next layer to be mixed in	local	y	y
$GA1_{E/O}$	$G_m(1)$		Value of polynomial for momentum at $\sigma = 1$	local	y	n
$GD1_{E/O}$	$G_s(1)$		Same for scalars	local	y	n
$GA1Z_{E/O}$	$\partial_\sigma G_m(1)$		Derivative of polynomial for momentum at $\sigma = 1$	local	y	n
$GD1Z_{E/O}$	$\partial_\sigma G_s(1)$		Same for scalars	local	y	n
$HBL_{E/O}$	h	m	Mixed-layer depth	global	y	y
$HBL_{E/O}MAX$	h_{max}	m	Maximum mixed-layer depth	local	y	y
$HBL_{E/O}MIN$	h_{min}	m	Minimum mixed-layer depth	local	y	y
HDEPTH	d	m	Depth	local	y	n
$KWU_{E/O}$	k		Mixed-layer identifier	global	y	y
$RHO_{E/O}$	ρ	kg/m^3	Auxiliary array for the density	local	n	y
$RMIX_{E/O}$	ρ_{mix}	kg/m^3	Mixed-layer density	local	n	y
SIGMA	σ		Nondimensional vertical coordinate in mixed layer	local	y	n
$SMIX_{E/O}$	S_{mix}	PSU	Mixed-layer salinity	local	n	y
$TK_{E/O}$	TKE	m^3/s^2	Turbulent kinetic energy	local	n	y
$TMIX_{E/O}$	T_{mix}	°C	Mixed-layer temperature	local	n	y
$UMIX_{E/O}$	U_{mix}	m/s	Mixed-layer zonal velocity	local	n	y
$USTAR_{E/O}$	u_*	m/s	Friction velocity in water	global	y	y
$VMIX_{E/O}$	V_{mix}	m/s	Mixed-layer meridional velocity	local	n	y
$WA_{E/O}$	w_m	m/s	Turbulent velocity scale for momentum	local	y	n
$WD_{E/O}$	w_s	m/s	Turbulent velocity scale for scalars	local	y	n
$WSA_{E/O}$	$\overline{wS}_0$	PSU m/s	Turbulent salinity flux	global	y	y
$WTH_{E/O}$	$\overline{w\theta}_0$	°C m/s	Turbulent temperature flux	global	y	y
$WUK_{E/O}$	$\overline{wu}_0$	m^2/s^2	Turbulent zonal velocity flux	global	y	y
$WVK_{E/O}$	$\overline{wv}_0$	m^2/s^2	Turbulent meridional flux	global	y	y

Table 7: Model variables (1-D, KE)

Name	Symbol	Units	Description	Type	N	B
PIN	P	Pa	Auxiliary array for pressure in EXPCOEF	local	y	n

Table 8: Model variables (Temporary, all local)

Name	Symbol	Units	Description	N	B
$AV1_{E/O}$	$A_V\|_{\sigma=1}$	m^2/s	Eddy viscosity coefficient at $\sigma = 1$	y	n
$AV1Z_{E/O}$	$\partial_\sigma A_V\|_{\sigma=1}$	m^2/s	Derivative of the eddy viscosity coefficient at $\sigma = 1$	y	n
$B_{E/O}AVG$	B_{avg}	m/s^2	Averaged buoyancy on layer interfaces	y	n

CCS	C_s		Proportionality coefficient parameterizing γ_s	y	n
D1$_{E/O}$	D_1	m	Modified thickness of second layer above bottom	y	n
D2$_{E/O}$	D_2	m	Modified thickness of first layer above bottom	y	n
DIFK$_{E/O}$	ΔKE	m^3/s^2	Gain of kinetic energy by mixing in a deeper layer	n	y
DIFP$_{E/O}$	ΔPE	m^3/s^2	Gain/loss of potential energy by mixing in a deeper layer	n	y
DIFTKE$_{E/O}$	ΔTKE	m^3/s^2	Gain/loss of total TKE by mixing in a deeper layer	n	y
DIFW$_{E/O}$	ΔWE	m^3/s^2	Dissipation of wind energy in a certain layer	n	y
DNEW	D_{new}	m	Next layer to be added to the mixed layer	y	y
DV1$_{E/O}$	$D_V\|_{\sigma=1}$	m^2/s	Eddy diffusivity coefficient at $\sigma = 1$	y	n
DV1Z$_{E/O}$	$\partial_\sigma D_V\|_{\sigma=1}$	m^2/s	Derivative of the eddy diffusivity coefficient at $\sigma = 1$	y	n
FAC$_{E/O}$	f		General fraction of next layer to be mixed in	y	y
FACHM$_{E/O}$	$f_{h_{max}}$		Fraction of next layer to be mixed in, from h_{max} condition	y	y
FACHN$_{E/O}$	$f_{h_{min}}$		Fraction of next layer to be mixed in, from h_{min} condition	y	y
FACRI$_{E/O}$	f_{Ri}		Fraction of next layer to be mixed in, from Ri condition	y	n
FACTK$_{E/O}$	f_{TKE}		Fraction of next layer to be mixed in, from TKE condition	n	y
FLAG$_{E/O}$			Flag, 0/1, stating if a general condition is unfulfilled/fulfilled	y	y
FLAGBF$_{E/O}$			Flag, 0/1, stating if the B_f condition is unfulfilled/fulfilled	y	n
FLAGHM$_{E/O}$			Flag, 0/1, stating if the h_{max} condition is unfulfilled/fulfilled	y	y
FLAGHN$_{E/O}$			Flag, 0/1, stating if the h_{min} condition is fulfilled/unfulfilled	y	y
FLAGRI$_{E/O}$			Flag, 0/1, stating if the Ri condition is unfulfilled/fulfilled	y	n
FLAGTK$_{E/O}$			Flag, 0/1, stating if the TKE condition is unfulfilled/fulfilled	n	y
GA$_{E/O}$	$G_m(d/h)$		Third degree polynomial for momentum	y	n
GD$_{E/O}$	$G_s(d/h)$		Third degree polynomial for scalars	y	n
HNEW	h_{new}	m	Depth of the base of D_{new}	y	y
HOLD	h_{old}	m	Depth of the top of D_{new}	n	y
HREF	h_{ref}	m	Reference level, close to the surface, used in (2.3)	y	n
KW$_{E/O}$	k		Mixed-layer identifier	y	n
PHIM, PHIS	ϕ_m, ϕ_s		Dimensionless flux profiles for momentum and scalars	y	n
RR$_{E/O}$	R		Ratio of the mixed-layer depth minus the top of the layer to the thickness of the layer	y	n
SFACTOR	f'		Fraction of next layer to be mixed in, modified in the case of partial mixing of velocities	n	y
SIGMAX	σ'		Nondimensional vertical coordinate in mixed layer, modified in the case of negative buoyancy forcing	y	n
U$_{E/O}$AVG	U_{avg}	m/s	Averaged zonal velocity on layer interfaces	y	n
V$_{E/O}$AVG	V_{avg}	m/s	Averaged meridional velocity on layer interfaces	y	n
VT2$_{E/O}$	V_t^2	m^2/s^2	Square of velocity scale of turbulent velocity shear	y	n
WAZ$_{E/O}$	$\partial_\sigma w_m\|_{\sigma=1}$	m/s	Derivative of turbulent velocity scale for momentum at $\sigma = 1$	y	n
WBRAD$_{E/O}$	$-B_R$	m^3/s^2	Radiative contribution to the surface buoyancy forcing B_f	y	n
WBTUR$_{E/O}$	$\overline{wb}_0$	m^3/s^2	Turbulent contribution to the surface buoyancy forcing B_f	y	n
WDZ$_{E/O}$	$\partial_\sigma w_s\|_{\sigma=1}$	m/s	Derivative of turbulent velocity scale for scalars at $\sigma = 1$	y	n
WIND$_{E/O}$	WE(d)	m^3/s^2	Wind energy at depth d	n	y
XN$_{E/O}$	N	s^{-1}	Brunt-Väisällä frequency	y	n
ZZ	ζ		Stability parameter, equal to du_*^3/B_f	y	n

Appendix B
Modifications to HOPE routines

The source of the added subroutine OCFLUX and the modified part of subroutine OCTHER are shown below. These modifications are needed to obtain the correct separation of the surface fluxes and the ocean forcing needed for the mixed-layer schemes. For brevity most comments have been left out.

The new routine OCFLUX saves the flux fields for the mixing routines.

```
SUBROUTINE OCFLUX
     *(
```

```
#include "dyn_outarg.h"
     *)
#include "dyn_outdim.h"
#include "param.h"
#include "commo1.h"
#include "oceval.h"
#include "relax.h"
#include "mixcom.h"
C--------------------------------------------------
      REAL FLD1E(IE,JE),FLD1O(IE,JE)
      REAL FLD2E(IE,JE),FLD2O(IE,JE)
      REAL SOLGLE(IE,JE,KE),SOLGLO(IE,JE,KE)

C-------------------- BUOYANCY FLUXES --------------
      RELTDZW  = RELTEM*DZW(1)
      RELSDZW  = RELSAL*DZW(1)
      RELTIDZW = RELTICE*DZW(1)
      RELSIDZW = RELSICE*DZW(1)
      DTDWI    = DT*DWI(1)

      DO 1100 J=1,JE
      DO 1100 I=1,IE
         WETE=MAX(0.,DDPE(I,J,1)/(DDPE(I,J,1)-EPPS))
         WETO=MAX(0.,DDPO(I,J,1)/(DDPO(I,J,1)-EPPS))

         WTHE(I,J)=-((1-WOCSCAE(J))*RELTDZW*
     .                        (TAFE(I,J)-THE(I,J,1))
     .            +    WOCSCAE(J) *AOHFLXE(I,J)/ROCP
     .                                      )*WETE
         WTHO(I,J)=-((1-WOCSCAO(J))*RELTDZW*
     .                        (TAFO(I,J)-THO(I,J,1))
     .            +    WOCSCAO(J) *AOHFLXO(I,J)/ROCP
     .                                      )*WETO
         WSAE(I,J)=-( RELSDZW*(SAFE(I,J)-SAE(I,J,1))
     .          - IAPME*AOPMEE(I,J)*SAE(I,J,1))*WETE
         WSAO(I,J)=-( RELSDZW*(SAFO(I,J)-SAO(I,J,1))
     .          - IAPME*AOPMEO(I,J)*SAO(I,J,1))*WETO

         THETMP = THE(I,J,1) - DTDWI*WTHE(I,J)
         THOTMP = THO(I,J,1) - DTDWI*WTHO(I,J)
         SAETMP = SAE(I,J,1) - DTDWI*WSAE(I,J)
         SAOTMP = SAO(I,J,1) - DTDWI*WSAO(I,J)

         FLAGTE=MIN(1.,(0.5+SIGN(0.5,TFREEZ-THETMP))
     .           + (0.5+SIGN(0.5,TFREEZ-TICE(I,J))))
     .                                    *ICEPSEUDO
         FLAGTO=MIN(1.,(0.5+SIGN(0.5,TFREEZ-THOTMP))
     .           + (0.5+SIGN(0.5,TFREEZ-TICO(I,J))))
     .                                    *ICEPSEUDO
         FLAGSE = (0.5+SIGN(0.5,TFREEZ-TICE(I,J)))
     .                                    *ICEPSEUDO
         FLAGSO = (0.5+SIGN(0.5,TFREEZ-TICO(I,J)))
     .                                    *ICEPSEUDO

         WTHE(I,J) = WTHE(I,J) - FLAGTE*RELTIDZW*
     .                        (TICE(I,J)-THETMP)*WETE
         WTHO(I,J) = WTHO(I,J) - FLAGTO*RELTIDZW*
     .                        (TICO(I,J)-THOTMP)*WETO
         WSAE(I,J) = WSAE(I,J) - FLAGSE*RELSIDZW*
     .                        (SICE(I,J)-SAETMP)*WETE
         WSAO(I,J) = WSAO(I,J) - FLAGSO*RELSIDZW*
     .                        (SICO(I,J)-SAOTMP)*WETO

         FLD1E(I,J) =-WTHE(I,J)*ROCP
         FLD1O(I,J) =-WTHO(I,J)*ROCP
         FLD2E(I,J) = WSAE(I,J)/SAE(I,J,1)
         FLD2O(I,J) = WSAO(I,J)/SAO(I,J,1)

1100  CONTINUE

      NLEV=1
      ICODE= 28 + 128  ! instant field
      CALL OUTPROC(FLD1O,FLD1E,NLEV,'V ',ICODE,
#include "dyn_outarg.h"
     *)
      NLEV = 1
      ICODE= 30+128   !instant field
      CALL OUTPROC(FLD1O,FLD1E,NLEV,'V ',ICODE,
#include "dyn_outarg.h"
     *)

C-------------------- SOLAR PENETRATION ------------
      DO 1200 K=1,KE
      DO 1200 J=1,JE
      DO 1200 I=1,IE
         SOLGLE(I,J,K) = SOLPROF(K)*ISOLPR
         SOLGLO(I,J,K) = SOLPROF(K)*ISOLPR
1200  CONTINUE

      SOLTRANS = 0.0

      DO 1210 K=1,KE-1
      SOLTRANS = SOLTRANS - SOLPROF(K)

      DO 1210 J=1,JE
      DO 1210 I=1,IE

         WETEO = MAX(0.,DDPE(I,J,K  )/(DDPE(I,J,K  )
     .                                      -EPPS))
         WETEU = MAX(0.,DDPE(I,J,K+1)/(DDPE(I,J,K+1)
     .                                      -EPPS))
         WETOO = MAX(0.,DDPO(I,J,K  )/(DDPO(I,J,K  )
     .                                      -EPPS))
         WETOU = MAX(0.,DDPO(I,J,K+1)/(DDPO(I,J,K+1)
     .                                      -EPPS))

         SOLGLE(I,J,K) = SOLGLE(I,J,K)
     .                 + SOLTRANS*WETEO*(1.-WETEU)
```

```
         SOLGLO(I,J,K) = SOLGLO(I,J,K)
     .                   + SOLTRANS*WETOO*(1.-WETOU)
1210  CONTINUE

      DO 1220 K=1,NSOLPEN
      DO 1220 J=1,JE
      DO 1220 I=1,IE

         WJE(I,J,K) =-AOSOLE(I,J)*SOLGLE(I,J,K)/ROCP
         WJO(I,J,K) =-AOSOLO(I,J)*SOLGLO(I,J,K)/ROCP

         IF (K.EQ.1)THEN
            FLD1E(I,J) = -ROCP*AOSOLE(I,J)
     .                           *(SOLGLO(I,J,1)+1.)
            FLD1O(I,J) = -ROCP*AOSOLO(I,J)
     .                           *(SOLGLE(I,J,1)+1.)
         ELSE
            FLD1E(I,J) = FLD1E(I,J)-ROCP*WJO(I,J,K)
            FLD1O(I,J) = FLD1O(I,J)-ROCP*WJE(I,J,K)
         ENDIF

1220  CONTINUE

      NLEV=1
      ICODE= 29+128   !instant field
      CALL OUTPROC(FLD1O,FLD1E,NLEV,'V ',ICODE,
#include "dyn_outarg.h"
     *)

C-------------------- WIND FLUXES ------------------
      DO 1300 J=1,JE
      DO 1300 I=1,IE

         WUKE(I,J)  = -AOTXE(I,J)*0.000977
         WUKO(I,J)  = -AOTXO(I,J)*0.000977
         WVKE(I,J)  = -AOTYE(I,J)*0.000977
         WVKO(I,J)  = -AOTYO(I,J)*0.000977

         FLD1E(I,J) = -WUKE(I,J)/0.000977
         FLD1O(I,J) = -WUKO(I,J)/0.000977
         FLD2E(I,J) = -WVKE(I,J)/0.000977
         FLD2O(I,J) = -WVKO(I,J)/0.000977

1300  CONTINUE

      NLEV=1
      ICODE= 25+128   !instant taux
      CALL OUTPROC(FLD1O,FLD1E,NLEV,'V ',ICODE,
#include "dyn_outarg.h"
     *)
      NLEV=1
      ICODE= 26+128   !instant tauy
      CALL OUTPROC(FLD2O,FLD2E,NLEV,'V ',ICODE,
#include "dyn_outarg.h"
     *)

C-----------------------------------------------
      RETURN
      END
```

Part A of OCTHER (boundary forcing on temperature, salt and sea level) also had to be modified. It is now coded as follows

```
SUBROUTINE OCTHER
     *(
#include "dyn_outarg.h"
     *)

#include "dyn_outdim.h"
#include "param.h"
#include "commo1.h"
#include "oceval.h"
#include "mixpar.h"
#include "relax.h"
#include "mixcom.h"
      COMMON /STACK1/ AAVE,AAVO
      REAL AAVE(IE,JE,KEP), AAVO(IE,JE,KEP)
      REAL RHUPPE(IE,JE),RHUPPO(IE,JE)
      REAL FLDE(IE,JE,KEP),FLDO(IE,JE,KEP)

C=================================================
C
C     A) FORCING FROM OCFLUX APLLIED TO FIELDS
C
C-------------------------------------------------
      DTDWI = DT*DWI(1)

      DO 1100 J=1,JE
      DO 1100 I=1,IE

         ZE(I,J) = ZE(I,J) + DT*WSAE(I,J)/SAE(I,J,1)
         ZO(I,J) = ZO(I,J) + DT*WSAO(I,J)/SAO(I,J,1)
         THE(I,J,1) = THE(I,J,1) - DTDWI*WTHE(I,J)
         THO(I,J,1) = THO(I,J,1) - DTDWI*WTHO(I,J)
         SAE(I,J,1) = SAE(I,J,1) - DTDWI*WSAE(I,J)
         SAO(I,J,1) = SAO(I,J,1) - DTDWI*WSAO(I,J)

1100  CONTINUE

      IF(ICYCLI.GE.1) CALL PERIO2(1,ZE)
      IF(ICYCLI.GE.1) CALL PERIO2(2,ZO)

C-------------------- SOLAR PENETRATION ------------
      DO 1200 K=1,KE

      DTDWI = DT*DWI(K)

      DO 1200 J=1,JE
```

```
      DO 1200 I=1,IE

         TRIE = ICEPSEUDO*TICE(I,J) + (1.-ICEPSEUDO)
     .                                  *THE(I,J,1)
         TRIO = ICEPSEUDO*TICO(I,J) + (1.-ICEPSEUDO)
     .                                  *THO(I,J,1)
         WETE=MAX(0.,DDPE(I,J,K)/(DDPE(I,J,K)-EPPS))
     .        * (0.5-SIGN(0.5,TFREEZ-TRIE))
         WETO=MAX(0.,DDPO(I,J,K)/(DDPO(I,J,K)-EPPS))
     .        * (0.5-SIGN(0.5,TFREEZ-TRIO))

         THE(I,J,K) = THE(I,J,K) - DTDWI*WJE(I,J,K)
     .                                          *WETE
         THO(I,J,K) = THO(I,J,K) - DTDWI*WJO(I,J,K)
     .                                          *WETO
1200  CONTINUE

      CALL OCPODI
C=====================================================
C
C     B)
C
C     BAROCLINIC PRESSURE AND STABILITY
...
```

Finally, OCWIND can be simplified as part of the work has already been done in OCFLUX.

```
SUBROUTINE OCWIND
     *(
#include "dyn_outarg.h"
     *)
#include "dyn_outdim.h"
#include "param.h"
#include "commo1.h"
#include "oceval.h"
#include "relax.h"
#include "mixcom.h"

      DTDWI = DT*DWI(1)

      DO 1 J=1,JE
      DO 1 I=1,IE

        AMSUE=MAX(0.,DDUE(I,J,1)/(DDUE(I,J,1)-EPPS))
     .     * (0.5-SIGN(0.5,TFREEZ-THE(I,J,1)))*IATAU
        AMSUO=MAX(0.,DDUO(I,J,1)/(DDUO(I,J,1)-EPPS))
     .     * (0.5-SIGN(0.5,TFREEZ-THO(I,J,1)))*IATAU

         UOE(I,J,1) = UOE(I,J,1) - DTDWI*WUKE(I,J)
     .                                        *AMSUE
         UOO(I,J,1) = UOO(I,J,1) - DTDWI*WUKO(I,J)
     .                                        *AMSUO
         VOE(I,J,1) = VOE(I,J,1) - DTDWI*WVKE(I,J)
     .                                        *AMSUE
         VOO(I,J,1) = VOO(I,J,1) - DTDWI*WVKO(I,J)
     .                                        *AMSUO
1     CONTINUE

      RETURN
      END
```

KNMI-PUBLICATIES, VERSCHENEN SEDERT 1995

Een overzicht van eerder verschenen publicaties, wordt verzoek toegezonden door de Bibliotheek van het KNMI, postbus 201, 3730 AE De Bilt, tel 030 - 2 206 855, fax. 030 - 2 210 407; e-mail: biblioth@knmi.nl

KNMI-PUBLICATIE MET NUMMER

150-28 Sneeuwdek in Nederland 1961-1990 / A.M.G. Klein Tank
176-S Stormenkalender: chronologisch overzicht van alle stormen (windkracht 8 en hoger) langs de Nederlandse kust voor het tijdvak 1990-1996 / [samenst. B. Zwart a.o.]
180a List of acronyms in environmental sciences : revised edition / [compiled by P. Geerders and M. Waterborg]
181b FM12 SYNOP internationale en nationale regelgeving voor het coderen van de groepen 7wwW1W2 en 960ww; derde druk
183-1 Rainfall in New Guinea (Irian Jaya) / T.B. Ridder
183-2 Vergelijking van zware regens te Hollandia (Nieuw Guinea), thans Jayapura (Irian Jaya) met zware regens te De Bilt / T. B. Ridder
183-3 Verdamping in Nieuw-Guinea, vergelijking van gemeten hoeveelheden met berekende hoeveelheden / T.B. Ridder
183-4 Beschrijving van het klimaat te Merauke, Nieuw Guinea, in verband met de eventuele vestiging van een zoutwinningsbedrijf / T.B. Ridder a.o.
183-5 Overzicht van klimatologische en geofysische publikaties betreffende Nieuw-Guinea / T.B. Ridder
184a Inleiding tot de algemene meteorologie : studie-uitgave , 2e druk / B. Zwart, A. Steenhuisen, m.m.v. H.J. Krijnen
185a Handleiding voor het gebruik van sectie 2 van de FM 13-X SHIP-code voor waarnemers op zee / KNMI; KLu; KM
186-I Rainfall generator for the Rhine Basin: single-site generation of weather variables by nearest-neighbour resampling / T. Brandsma and T.A. Buishand
187 De wind in de rug: KNMI-weerman schaatst de Elfstedentocht / H. van Dorp

TECHNISCH RAPPORT = TECHNICAL REPORT (TR)

168 Analyse van het seismische risico in Noord-Nederland / Th. de Crook a.o.
169 Evaluatie van neerslagprognoses van numerieke modellen voor de Belgische Ardennen in december 1993 / Erik van Meijgaard
170 DARR-94 / C.P.G. Lomme
171 EFEDA-91: documentation of measurements obtained by KNMI / W.A.A. Monna a.o.
172 Cloud lidar research at the Royal Netherlands Meteorological Institute KNMI2B2, version 2 cloud lidar analysis / A.Y. Fong a.o.
173 Measurement of the structure parameter of vertical wind-velocity in the atmospheric boundary layer / R. van der Ploeg
174 Report of the ASGASEX'94 workshop / ed. by W.A. Oost
175 Over slecht zicht, bewolking, windstoten en gladheid / J. Terpstra
176 Verification of the WAQUA/CSM-16 model for the winters 1992-93 and 1993-94 / J.W. de Vries
177 Nauwkeuriger nettostraling meten / M.K. van der Molen en W. Kohsiek
178 Neerslag in het stroomgebied van de Maas in januari 1995: waarnemingen en verificatie van modelprognoses / R.Jilderda a.o.
179 First field experience with 600PA phased array sodar / H. Klein Baltink
180 Een Kalman-correctieschema voor de wegdektemperatuurverwachtingen van het VAISALA-model / A. Jacobs
181 Calibration study of the K-Gill propeller vane / Marcel Bottema
182 Ontwikkeling van een spectraal UV-meetinstrument / Frank Helderman
183 Rainfall generator for the Rhine catchment : a feasibility study / T. Adri Buishand and Theo Brandsma
184 Parametrisatie van mooi-weer cumulus / M.C. van Zanten
185 Interim report on the KNMI contributions to the second phase of the AERO-project / Wiel Wauben, Paul Fortuin a.o.
186 Seismische analyse van de aardbevingen bij Middelstum (30 juli 1994) en Annen (16 augustus '94 en 31 januari '95) / [SO]
187 Analyse wenselijkheid overname RIVM-windmeetlokaties door KNMI / H. Benschop
188 Windsnelheidsmetingen op zeestations en kuststations: herleiding waarden windsnelheden naar 10-meter niveau / H. Benschop
189 On the KNMI calibration of net radiometers / W. Kohsiek
190 NEDWAM statistics over the period October 1994 - April 1995 / F.B. Koek
191 Description and verification of the HIRLAM trajectory model / E. de Bruijn
192 Tiltmeting · een alternatief voor waterpassing ? / H.W. Haak
193 Error modelling of scatterometer, in-situ and ECMWF model winds; a calibration refinement / Ad Stoffelen
194 KNMI contribution to the European project POPSICLE / Theo Brandsma a.o.
195 ECBILT a coupled atmosphere ocean sea-ice model for climate predictability studies / R.J. Haarsma a.o.
196 Environmental and climatic consequences of aviation: final report of the KNMI contributions to the AERO-project / W. Wauben a.o.
197 Global radiation measurements in the operational KNMI meteorological network: effects of pollution and ventilation / F. Kuik
198 KALCORR: a kalman-correction model for real-time road surface temperature forecasting / A. Jacobs
199 Macroseismische waarnemingen Roswinkel 19-2-1997 / B. Dost e.a.
200 Operationele UV-metingen bij het KNMI / F. Kuik
201 Vergelijking van de Vaisala's HMP233 en HMP243 relatieve luchtvochtigheidsmeters / F. Kuik
202 Statistical guidance for the North Sea / Janet Wijngaard and Kees Kok
203 UV-intercomparison SUSPEN / Foeke Kuik and Wiel Wauben
204 Temperature corrections on radiation measurements using Modtran 3 / D.A. Bunskoek, A.C.A.P. van Lammeren and A.J. Feijt
205 Seismisch risico in Noord-Nederland / Th. De Crook, H.W. Haak en B. Dost
206 The HIRLAM-STAT-archive and its application programs / Albert Jacobs
207 Retrieval of aerosol properties from multispectral direct sun measurements / O.P. Hasekamp
208 The KNMI Garderen Experiment, micro-meteorological observations 1988-1989; instruments and data / F.C. Bosveld, J.G. van der Vliet and W.A.A. Monna.
209 CO2 in water and air during ASGAMAGE: concentration measurements and consensus data / Cor M.J. Jacobs, Gerard J. Kunz, Detlev Sprung a.o.
210 Elf jaar Cabauw-metingen / J.G. van der Vliet
211 Indices die de variabiliteit en de extremen van het klimaat beschrijven / E.J. Klok
212 First guess TAF-FGTAF: semi-automation in TAF production / Albert Jacobs
213 Zeer korte termijn bewolkingsverwachting met behulp van METCAST: een verificatie en beschrijving model-uitvoer / S.H. van der Veen

WETENSCHAPPELIJK RAPPORT = SCIENTIFIC REPORT (WR)

95-01 Transformation of precipitation time series for climate change impact studies / A.M.G. Klein Tank and T.A. Buishand
95-02 Internal variability of the ocean generated by a stochastic forcing / M.H.B. van Noordenburg
95-03 Applicability of weakly nonlinear theory for the planetary-scale flow / E.A. Kartashova
95-04 Changes in tropospheric NOx and o3 due to subsonic aircraft emissions / W.M.F. Wauben a.o.
95-05 Numerical studies on the Lorenz84 atmosphere model / L. Anastassiades
95-06 Regionalisation of meteorological parameters / W.C. de Rooy
95-07 Validation of the surface parametrization of HIRLAM using surface-based measurements and remote sensing data / A.F. Moene a.o.
95-08 Probabilities of climatic change · a pilot study / Wieger Fransen (ed.) a.o.
96-01 A new algorithm for total ozone retrieval from direct sun measurements with a filter instrument / W.M.F. Wauben
96-02 Chaos and coupling: a coupled atmosphere ocean-boxmodel for coupled behaviour studies / G. Zondervan
96-03 An acoustical array for subsonic signals / H.W. Haak
96-04 Transformation of wind in the coastal zone / V.N. Kudryavtsev and V.K. Makin
96-05 Simulations of the response of the ocean waves in the North Atlantic and North Sea to co2 doubling in the atmosphere / K. Rider a.o.
96-06 Microbarograph systems for the infrasonic detection of nuclear explosions / H.W. Haak and G.J. de Wilde
96-07 An ozone climatology based on ozonesonde measurements / J.P.F. Fortuin
96-08 GOME validation at KNMI and collaborating institutes / ed. by P. Stammes and A. Piters
97-01 The adjoint of the WAM model / H. Hersbach
97-02 Optimal interpolation of partitions: a data assimilation scheme for NEDWAM-4; description and evaluation of the period November 1995 - October 1996 / A.Voorrips
97-03 SATVIEW: a semi-physical scatterometer algorithm / J.A.M. Janssen and H. Wallbrink
97-04 GPS water vapour meteorology · status report / H. Derks, H. Klein Baltink, A. van Lammeren, B. Ambrosius, H. van der Marel ao.
97-05 Climatological spinup of the ECBILT oceanmodel / Arie Kattenberg and Sybren S. Drijfhout
97-06 Direct determination of the air-sea transfer velocity of co2 during ASGAMAGE / J.C.M. Jacobs, W Kohsiek and W.A. Oost
97-07 Scattering matrices of ice crystals / M. Hess, P Stammes and R.B.A. Koelemeijer
97-08 Experiments with horizontal diffusion and advection in a nested fine mesh mesoscale model / E.I.F. de Bruijn
97-09 On the assimilation of ozone into an atmospheric model / E.Valur Hólm
98-01 Steady state analysis of a coupled atmosphere ocean-boxmodel / F.A. Bakker
98-02 The ASGAMAGE workshop, September 22-25, 1997 / ed. W.A. Oost
98-03 Experimenting with a similarity measure for atmospheric flows / R.A. Pasmanter and X.-L. Wang
98-04 Evaluation of a radio interferometry lightning positioning system / H.R.A. Wessels
98-05 Literature study of climate effects of contrails caused by aircraft emissions / V.E. Pultau